Cláudia Filipa Cunha Antunes

Relevance of tissue macrophages in lung development

Cláudia Filipa Cunha Antunes

Relevance of tissue macrophages in lung development

UMinho | 2013

Universidade do Minho
Escola de Ciências da Saúde

Cláudia Filipa Cunha Antunes

Relevance of tissue macrophages in lung development

Setembro de 2013

Universidade do Minho
Escola de Ciências da Saúde

Cláudia Filipa Cunha Antunes

Relevance of tissue macrophages in lung development

Master Thesis
Master in Health Sciences

This work was performed under supervision of
Sandra Maria Araújo Costa, PhD

Setembro de 2013

ACKNOWLEDGMENTS

Acknowledgments

Não construimos uma tese sozinhos, embora muito do que apresentamos no final seja não mais do que o somatório de muitos momentos de luta connosco próprios.

Ainda assim, há pessoas cujo empenho e companheirismo salutares merecem um especial agradecmento.

Á minha orientadora Sandra Costa, deixo a minha sincera gratidão pela orientação, dedicação, pela extrema fibra que foi demonstrando sempre que surgiam problemas e não foram poucos. Porque começamos a construír tudo do zero com tudo o que isso implica.

À comissão organizadora do mestrado em Ciências da Saúde, pela oportunidade que me deu de o poder integrar.

A todo o ICVS – Instituto de Investigação de Ciências da Vida e da Saúde, em particular ao Domínio das Ciências Cirúrgicas.

Ao laboratório de Oncologia onde fiquei grande parte da tese e que muitas vezes auxiliou nas minhas pequenas/grandes dúvidas (Vera,Filipa, Susana,Céline, Ricardo A. e Ricardo C.).

Ao laboratório de Desenvolvimento, onde encontrei a Sheeba, Raquel, AnaLuce, Hugo, Duda.

Á Marina S. pelos PCR's, pelas imunos, pela tua ajuda Voluntária!

À Cristina e Marina A., minhas companheiras das intermináveis horas de estereologia!

Aos serviços de Histologia e Biologia Molecular, pelo apoio técnico, Miguel, Luís e Goreti muito obrigada!

À minha família e amigos. Aos meus pais por financiarem o meu trabalho durante este tempo e por muito mais.. À minha irmã. Às minhas amigas de todo o sempre: Susana e Francisca. Aos meus amigos de muitos anos: Zé, Sílvia, Guida, Marta e Carla.

Abstract

Macrophages are found in almost every tissue, from embryonic to adulthood, with trophic roles during development. In organs such as brain, kidney, mammary gland and pancreas, macrophages reside in considerable number and provide important regulatory functions that shape their development and maturation. Some studies have demonstrated the regulation of developmental morphogenesis by macrophages, more specifically in vascular system formation and branching morphogenesis. Lung is a branching organ and its morphogenesis is dependent on interactions between epithelial and endothelial compartments. Indeed, in fetal lung, macrophages represent around 2-5% of the total lung cells. However, their precise contribution to lung development remains unknown. In this way, the main goal of this work was to unfold the functional role of tissue macrophages on lung development. Therefore, we aimed to understand whether and how macrophage ablation impaired fetal and neonatal lung development, using a macrophage-deficient mouse model ($Csf1r^{-/-}$ mice). The first aim was to characterize lung morphology of $Csf1r^{-/-}$ versus wild type and $Csf1r^{+/-}$ mice. We performed lung stereological analysis (calculation of mesenchymal, epithelial and air space volume density (VD)) at pseudoglandular (embryonic day (E) 15.5), fetal saccular (E18.5) and at post-natal saccular (after birth, P0) developmental stages. The lung mesenchymal VD in $Csf1r^{+/-}$ and $Csf1r^{-/-}$ mice was increased when compared with wild type mice in all stages analysed. At E18.5, beyond an increase in lung mesenchymal, a decrease of epithelial and airspace VD was observed in $Csf1r^{-/-}$ mice. Finally, at P0 stage, $Csf1r^{-/-}$ derived lungs showed a decrease in bronchiolar and air space VD as well as an increase in the mesenchymal VD compared with control group. These results suggested a delay in lung morphogenesis associated with macrophage tissue ablation. Keeping in mind that macrophages support angiogenesis during organ development and remodelling, we assessed vessel density on lungs, by immunohistochemical analysis of CD31 endothelial cell marker. At P0, lungs from $Csf1r^{-/-}$ mice presented a significant decrease in vessel density when compared with wild type mice (p value=0.020). This finding demonstrates a deficiency in lung vascular network associated with macrophage ablation. Furthermore, we quantified RNA expression levels of key angiogenic factors (VEGF-A, Flk-1, Ang-1, Ang-2, Hif-1a and Fgf2) in lung from the different mice groups at E15.5, E18.5 and after birth, P0. At E15.5 stage, an up regulation of VEGF-A, Flk-1, Ang-2 and Fgf2 transcripts was found. At E18.5 a significant reduction of VEGF-A and Ang-2

RNA levels was demonstrated in Csf1r$^{+/-}$ and Csf1r$^{-/-}$ groups when compared with wild type lungs. However, the opposite trend was observed in P0 knockouts lungs, with an increase in VEGF-A, Flk-1, Ang-1 and Ang-2 transcripts expression levels. This could be explained by compensation mechanisms trying to reverse the deficient lung vasculature (less vessels) observed at P0. In conclusion, all these evidences demonstrate that macrophage ablation is critical to lung development, impairing airway epithelial and vascular compartments.

Resumo

Os macrófagos estão presentes em quase todos os tecidos desde a fase embrionária até à fase adulta, associados a funções tróficas durante o desenvolvimento. Em órgãos como cérebro, rim, glândula mamária e pâncreas, os macrófagos estão presentes em largo número, regulando o desenvolvimento da sua forma e maturação. A literatura tem demonstrado que processos da morfogénese do desenvolvimento como a ramificação e a formação do sistema vascular são altamente regulados pelos macrófagos. E o pulmão é também um órgão de ramificação, dependente da inter-ligação entre a componente epitelial e endotelial. Durante o desenvolvimento fetal deste órgão, os macrófagos representam cerca de 2 a 5 % do número total de células, permanecendo por identicar qual a sua relevância. Neste sentido, o objectivo deste trabalho foi perceber se e como a deleção dos macrófagos influência o desenvolvimento fetal e neo-natal do pulmão, usando um modelo de ratinho com a ablação dos macrófagos ($Csf1r^{-/-}$ ratinho). O nosso primeiro alvo de estudo foi caracterizar a morfologia dos pulmões que provêm de animais $Csf1r^{-/-}$ por comparação com os $Csf1^{+/-}$ e a estirpe selvagem. Desse modo, recorremos a análises esterológicas para calcular a densidade de volume (DV) de uma série de parâmetros como mesênquima, epitélio, espaço aéreo, em pontos específicos do desenvolvimento; no estadio pseudoglandular (desenvolvimento embriónico (E) 15.5), fetal sacular (E18.5) e pós-natal sacular (depois do nascimento, P0). A tendência observada sugere que os pulmões dos ratinhos $Csf1r^{-/-}$ e $Csf1r^{+/-}$ apresentam um aumento da densidade de volume de mesênquima quando comparado com o grupo controlo em todos os estadios. Especificamente a E 18.5, para além da densidade de volume de mesênquima estar aumentada, um decréscimo do epitélio e espaço aéreo foi observado para os $Csf1r^{-/-}$ animais. Por último, logo após o nacimento (estadio P0), os animais $Csf1r^{-/-}$ apresentaram uma diminuição da DV do epitélio bronquiolar e do espaço aéreo comparando com a estirpe selvagem. Estes resultados sugerem um atraso na morfogénse pulmonar associado à deleção dos macrófagos tecidulares. Por outro lado, a regulação dos macrófagos no processo angiogénico durante o desenvolvimento e no processo de remodelação dos vasos, suportou o seguinte foco de estudo. Nós analisamos a densidade dos vasos pulmonares, utilizando o marcador endotelial CD31, por imunohistoquímica. A P0, os pulmões dos animais com o genótipo $Csf1r^{-/-}$ apresentaram um decréscimo significativo comparado com o grupo controlo ($p=0.020$). Estes resultados demonstram uma deficiência na rede vascular

associado com a ablação dos macrófagos. Mais, avaliamos os níveis de expressão de RNA de factores angiogénicos chave como VEGF-A, Flk-1, Ang1, Ang2, Hif-1a e Fgf2, nos pulmões dos diferentes grupos de animais, a E15.5, E 18.5 e P0. A E 15.5 um aumento de VEGF-A, Flk-1, Ang-2 e Fgf2 foram encontrados. A E18.5, um decréscimo nos niveis de expressão de VEGF-A e Ang-2 para os animais $Csf1r^{+/-}$ and $Csf1r^{-/-}$ foi demonstrado. Mas quando avaliamos estes factores no estadio P0, um aumento significativo de VEGF-A, Flk-1, Ang-1 e Ang-2 foram encontrados comparando com o grupo controlo. Este resultado pode dever-se há existência de mecanismos compensatórios que tentam reverter a dificiente vasculaura (menor número de vasos) a P0. Em conclusão, estas evidências demonstram que a deleção dos macrófagos é critica para o desenvolvimento do pulmão, resultando no dano do epitélio das vias aéreas e da vasculatura.

TABLE OF CONTENTS

TABLE OF CONTENTS

ABBREVIATION LIST

Abbreviation List

Ang: Angiopoietin

Arg1: Arginase 1

BDP: Bronchopulmonary Dysplasia

Ccl17: Chemokine C-C motif ligand 17

cDNA: complementary Deoxyribonucleic Acid

Csf1: Colony stimulated factor

Csf1r: Colony stimulated factor receptor

CCSP: Clara Cell Secretory Protein

DAB: 3,3'-diamino-benzidine

ECs: Endothelial Cells

E: Embryonic Day

ECM: Extracellular Matrix

EDTA: Ethylenediamine Tetraacetic Acid

FGF: Fibroblast Growth Factor

Flk-1: Fetal Liver Kinase 1

GAPDH: Glyceraldehyde 3-Phosphate Dehydrogenase

GM-CFU: Granulocyte/Macrophage Colony-Forming Unit

GnRH: Gonadotropin-Releasing Hormone

H_2O_2: Hydrogen Peroxide

HIF-1a: Hypoxia-inducible Factor

IL: Interleukin

IPA: Isopropanol

IGF: Insulin-like Growth Factor

JAK/STAT: Janus Kinase/Signal Transducer and Activator of Transcription

LH: Luteinizing Hormone

LIF: Leukaemia Inhibitory Factor

LPS: Lipopolysaccharides

MAPK: Mitogen-Activated Protein Kinases

MDV: Microvessel Density

MIN: Minute

mmHg: Millimeter of Mercury

MPS- Mononuclear Phagocyte System

Mrc1: Mannose receptor 1

M1: Classically activated macrophages

M2: Alternative activated macrophages

NF-KB: Nuclear Factor kappa-light-chain-enhancer of activated B cells

P: Partial pressure

PBS: Phosphate Buffered Saline

PCR: Polymerase Chain Reaction

PECAM: Platelet Endothelial Cell Adhesion Molecule

PFA: Paraformaldehyde

PH: Pulmonary Hypertension

PPSCs: Bone marrow stem cells

PI3K: Phosphatidylinositol 3-kinase

qRT-PCR: Quantitative Reverse Transcription Polymerase Chain Reaction

RANKL: Receptor Activator of Nuclear factor-kB Ligand

RT: Room Temperature

RTKs: Protein-Tyrosine Kinase Receptors

Sat: Saturation

Shh: Sonic hedgehog

SEC: Second

STAT: Signal Transducers and Activators of Transcription

SP-C*:* Surfactant Protein C

SZ: Subventricular Zone

TEBs: Terminal End Buds

TGF-β- Transforming Growth Factor-β

TNF-α: Tumor Necrosis Factor

VD: Volume Density

VEGF: Vascular Endothelial Growth Factor

VEGFR: Vascular Endothelial Growth Factor Receptor

Wnt: Derived from Drosophila *Wingless* and the mouse *Int*

Figures and Tables

INTRODUCTION

1. INTRODUCTION

1.1. Lung development

Lung development is a highly regulated process. Its development is coordinated from the primary bud stage until the generation of millions of alveolar gas exchange units [1]. This process arises from embryogenesis and continues after birth which involves structural organization and functional maturity [2]. Gas exchange allows the oxygenation of red blood cells in the circulatory system and the simultaneous removal of carbon dioxide, being one of the most important characteristics of respiratory system [3]. Until the lung is fully capable to play this process a complex development program should take place. Mammalian lung development starts with the differentiation of ventral foregut endoderm into various epithelial cell types that contour the inner surface of the trachea and two primary buds, the primordial lung[4]. The endoderm gives rise to multiple resident epithelial cells and the mesoderm to vascular structures, airway smooth muscle and others [5]. After the primary lung buds formation, the two main bronchi of the primordial lung extend into the surrounding mesenchyme and begin the process of branching morphogenesis [1, 6]. The two main bronchi of the primordial lung are subdivided into sequentially finer buds, the bronchioles, which are surrounded by parabronchial smooth muscle, originating the common respiratory tree. This process is essential to elaborate the orchestration of the bronchioles and their endings, alveoli, highly specialized structures that allow gas exchange process. The branching program of the lung epithelium is accompanied at the same time by the development of the pulmonary vasculature, constituted by a blood vessels network, which covers the alveoli [1, 4]. It is the tight connection between the airways and the blood vessels the key for dynamic and complex respiratory process, which allows an efficient gas exchange.

1.1.2 Mouse and Human lung developmental stages

In Humans, the initiation of pulmonary development arises as a bifurcation at the posterior end of the laryngotracheal groove, occuring at 3-4 weeks of gestation. In rodents, the two buds that will originate right and left lung arise from the foregut endoderm, appearing on embryonic day (E) 9.5 of embryo development [2, 7]. Each lung bud develops into left and right lungs [2]. In both, humans and mice, lung constitution is asymmetrical. In humans, left lung

comprises two lobes while the right lung consists of three lobes. On the other hand, the left mice lung presents a single lobe and the right lung is composed of four lobes [6].

In both species, the embryological development of respiratory system can be divided into five principal stages (figure 1). In mouse, the first stage corresponds to lung primordium appearance (E8-9); followed by pseudoglandular stage, during which the primary buds generate a complex tree-like structure (E10-16); canalicular stage, where the terminal buds become narrower (E16-18); saccular stage, which involves the developing of numerous small sacs that are the precursors of the alveoli (E18.5 to postnatal day (P) 5); and lastly, alveolar stage (starts at birth and extends almost 4 weeks into postnatal life) associated with the increase of terminal saccules, alveolar ducts, and alveoli. In human embryos, during the embryonic period a pulmonary protuberance containing two buttons develops, with the formation of the trachea and bronchus (3-4 weeks); pseudoglandular period, during which organogenesis occurs allowing the complete formation of bronchial tree and the airways (5-17 weeks); canalicular period, when respiratory bronchiole appears and vascular network increases (16-26 weeks); saccular period, with expansion of air spaces (24-38 weeks) and alveolar period, when alveolar development occurs by the formation of secondary and tertiary septa (36 weeks-2years). For human the first four stages take place in utero and the last ends after birth. In mice, the fourth stage ends after birth and the last occurs exclusively after birth [1, 2, 8].

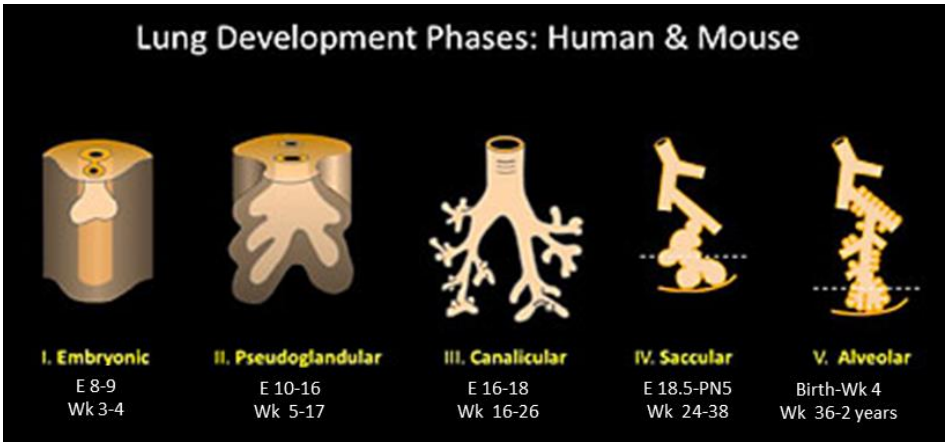

Figure 1. Principal stages of lung development in mouse and human: diagrammatic representations of the timeline and developmental organization (adapted from[9]).

1.1.3. Cellular Differentiation of the Lung

In mice, the current model of epithelial development describes that airway branching morphogenesis occurs during the pseudoglandular stage. The terminal buds contain a pool of highly proliferative multipotent progenitor cells, which give rise to several types of cells [1]. The differentiated airway tree is composed by a complex and large number of cells, which change significantly along the proximal-distal regions (**figure 2**). In adult mice, the proximal pseudostratified epithelium, composed by large airways (tracheobronchial region) shows three major cell types: ciliated, basal and clara secretory cells. Ciliated cells are first detected in the trachea and mainstem bronchi at approximately E14, being typically marked by expression of *FoxJ1* transcription factor. Basal cells are observed in the trachea at E10.5 associated with expression of the transcription factor *Trp63.* Clara cells are typically marked by synthesis of the secretoglobin family member Scgb1a1, (also known as CC10 or CCSP), which appears around E17 [1, 10, 11]. Concerning distal columnar epithelium, composed by small airways (intralobar bronchioles), the cell population is similar to the large airways, with no basal cells and more number of ciliated cells, neuroendocrine cells and Clara cells. Neuroendocrine cells are among the first cells to differentiate within the respiratory epithelium, with the starts of Dll1 expression at E13.5[1] [10]. During the canalicular and saccular stages, the terminal or acinar tubes narrow and give rise to small saccules and the walls of these sacs, the primary septae.

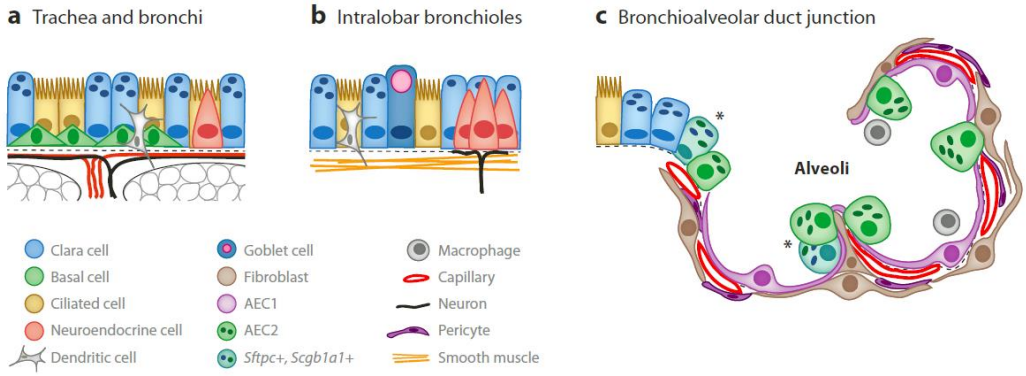

Figure 2. Cell types of the respiratory system. (*a*) Large airways (tracheobronchial region) are covered by a pseudostratified epithelium composed of basal cells, ciliated and secretory cells. (*b*) Small airways (intralobar bronchioles) a columnar epithelium containing ciliated, neuroendocrine and Clara cells. (*c*) The alveoli are composed by epithelial type 1 cells (AEC1) and cuboidal AEC2 cells and few cells secreting secretoglobulina Scgb1a1 (asterisks). The alveolar epithelial cells are closely associated with mesenchymal cells such as fibroblasts, endothelial cells and pericytes[10].

The endoderm begins to differentiate into the two main specialized cell types: type 1 and type 2 alveolar epithelial cells (AEC1 and AEC2) [10]. The type 1 cells constitute about 95% of the alveolar epithelium and lining the alveolar saccules, characteristically express aquaporin 5 and T1alpha. The type 2 cells comprise 5-10% of the alveolar surface and are characterized by production of surfactant-associated protein C (Sftpc or SPC) [5, 7]. Alveolar epithelial cells are closely associated with mesenchymal cells including fibroblasts, vascular smooth muscle cells, endothelial cells, vascular pericytes and macrophages [1].

1.1.4. Development of the Pulmonary Vasculature

The vascular development takes place throughout lung development with alterations in the structure of the capillary network. During mouse development, the vascular network of the lung is established from E≈10.5 and remains to develop postnatally. This system is composed of endothelial cells surrounded by vascular smooth muscle, pericytes, and other mesenchymal cells. All these cellular components are specifically organized to ensure the precise function of pulmonary vascular system [12]. Particularly, inhibition of lung endothelial cell development is accompanied by inhibition of airway epithelial cell differentiation and maturation [13]. Moreover, although significant airway remodeling occurs postnatally, the primary vascular network is established early in development, being essential for viability at birth [12]. Therefore, the crosstalk between the developing vasculature and the developing airways is a key event during lung development.

The angiogenesis and vasculogenesis are the crucial processes, which allow the lung vascular development since early stages [13]. Vasculogenesis is characterized to take place at early stages of embryo development, with a formation of new blood vessels *de novo*. On the other hand, angiogenesis promotes blood vessel formation from extension of pre-existing ones [14].
Concerning molecular players of pulmonary vasculature development, the pathways VEGF/VEGFR, Angiopoietin/TIE, Ephrins/Eph receptors, and Notch/Jagged appear to be essential in the regulation of pulmonary vascularization [15]. For instance, Ephrin B2 expressed by the microvasculature is critical for lung alveolization and secondary septae formation [16] [17]. Little is known about angiopoetins (Ang) expression during development, but for instance, overexpression of Ang-1 causes severe pulmonary hypertension and is increased in lungs from human patients with pulmonary hypertension [18]. Regarding Notch/Jagged pathway, for instance *Notch-1* and *Jagged-1* gene expression increased progressively from early to later lung

development, on vascular and nonvascular cells, suggesting their contribution during lung development. [19]. VEGF-A/VEGFR-2 signaling is a crucial pathway, which regulates physiological and pathological lung formation. This pathway has central action on vascular system, as a mitogen, survival, and differentiation factor for endothelial cells [20]. However, their relevance has been also demonstrated in pulmonary epithelial morphogenesis. For instance, in neo-natal mice, the neutralization of VEGF-A or VEGFR-2 (Flk-1) leads to a lung immature with less complex alveolar [21].

Furthermore, using mouse embryonic lung cultures treated with an antisense oligodeoxynucleotide to the VEGFR-2 was observed the loss of VEGF function which leads to a decreased in epithelial branching, epithelial and mesenchymal proliferation, and a downregulation of BMP-4 expression, an important regulator of lung development [22]. On the other hand, VEGF-A stimulation increases epithelial branching morphogenesis on lung embryonic cultures with an increases of Sp-c as well as Bmp-4 mRNA levels [22]. VEGF-A hyper expression in respiratory epithelium mice leads to lung vasculature alteration associated with disruption of the lung acinar structure, branching morphogenesis and inhibition of Type I cell differentiation [23]. These observations indicate that lung morphogenesis is critically dependent on lung neovascularization and VEGF/ VEGFR-2 pathway plays a key role in lung patterning. Together all these evidences demonstrated the close link between airway and vascular development, since the disruption of one system has critical consequences on the development of the other, and the other way around.

1.2. Macrophages

1.2.1. Macrophage origin and differentiation

Macrophages belong to the mononuclear phagocyte system (MPS). It includes bone-marrow-derived precursor cells, monocytes present in the peripheral blood and mature macrophages existent in the tissues [24]. Macrophages are normally identified in murine tissues using the markers, CD68, F4/80 and/or CD11b [25]. CD68, whose expression is restricted to mononuclear phagocytes, is a lysosomal antigen expressed (at high levels) in monocyte/macrophages [26]. F4/80 is a well-characterized membrane protein and the best known marker for mouse macrophages and blood monocytes [27]. CD11b is a leukocyte-specific receptor and is regarded as a marker for monocyte/macrophages, granulocytes, and natural

killer cells[28] In mice, the first population of macrophages is found in the late head-fold stage at E7.5 and has maternal origin [29]. However, the first embryonic macrophages, which derive from the primitive endoderm of the yolk sac, are found at E8 and sprout to the anterior structures of the embryo and don't express mature macrophage markers, such as F4/80. These macrophages don't differentiate from monocyte cells but directly from mesenchymal progenitor cells [30]. The first site of definite haematopoiesis is the yolk sac, followed at E10 by the aorta–gonads–mesonephros region of the embryo, where the second pool of hematopoietic progenitor cells and F4/80 positive cells are found [31-33]. By E10.5 to E11 the primitive liver becomes the principal site of haematopoiesis and from this moment, macrophages that have differentiated from monocytic progenitor cells colonize the entire embryo [32, 33]. After birth, the bone structures are formed and the bone marrow becomes the main site of haematopoiesis and the MPS is established [34]. Macrophages derive from pluripotent hematopoietic stem cells under the influence of numerous factors. The bone marrow stem cells (BMSCs) differentiate in multiple macrophages progenitor stages: from granulocyte/macrophage colony-forming unit (GM-CFU) to macrophage CFU (M-CFU) to monoblast to pro-monocyte and for last macrophage [24]. Transcription factors as PU.1 are important to macrophage differentiation. However, this is required only for macrophages differentiation from monocyte precursor, once PU.1-deficient mice is normal until the macrophages differentiation through the monocyte precursor starts [35] [32]. However, others factors are necessary for the differentiation of each macrophages cells precursors. The production of macrophages by the liver, and then by the bone marrow, is controlled in large part by the growth factor macrophage colony-stimulating factor (CSF-1). This growth factor allows the differentiation of macrophages from monocytes as well as their proliferation and viability *in vitro* [24]. Circulating CSF-1 is produced by endothelial cells in blood vessels and, together with locally produced CSF-1, regulates the survival, proliferation and differentiation of mononuclear phagocytes and osteoclasts (**figure 3**) [36].

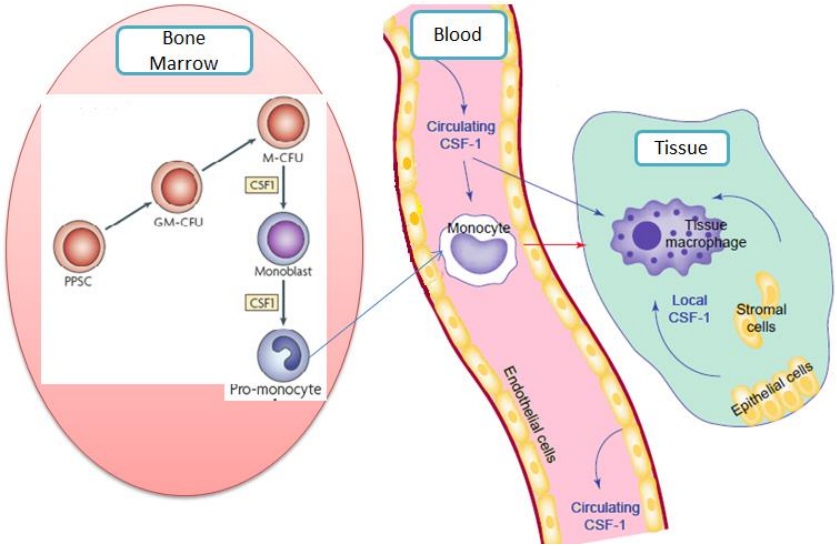

Figure 3. Macrophage origin and differentiation. Progenitors cells of MPS system arise from bone marrow, where from pluripotent stem cells (PPSCs) others progenitor are formed. The multipotent progenitors are granulocyte/macrophage colony-forming unit (GM-CFU), which differentiate in monoblast and this last in pro-monocyte. In blood vessels, endothelial cells produce CSF-1, which allows the differentiation of pro-monocyte coming from the bone marrow in monocytes. In the tissues, local produced CSF-1 allows the differentiation of monocytes in tissue macrophages. (Adapted from [24, 36])

1.2.2. CSF1/CSF1R Pathway

Csf-1 acts on its target cells by binding to colony stimulating factor 1 receptor (Csf1r), a cell-surface tyrosine kinase receptor expressed in macrophages and all trophoblast cell lineages [31]. The activation of this pathway is allowed by the link of Csf1 to the receptor Csf1r, which triggers their autophosphorylation and successive phosphorylation of downstream molecules. Phosphorylation of most of tyrosine residues creates docking sites for a variety of signaling molecules such as the p85 regulatory subunit of phosphatidylinositol 3-kinase (PI3K), Casitas B lineage (Cbl) and Grb2-associated binder-3 (Gab3), to mediate macrophage survival, differentiation, morphology and motility **(Figure 4)** [37-39]. Beyond Csf1, macrophages can also be grown and differentiated from monocytic progenitors in the presence of GM-CSF and to a lesser extent under the action of IL-3. The double action of these two factors allows the generation of mature macrophages [40, 41]. Mice with null mutation in the Csf1 gene or with null mutation in Csf1r are both deeply depleted of most macrophage populations. However, these mice are not totally depleted of macrophages, as is the case of spleen resident macrophages, thymus and lymph nodes derived-macrophages [36, 42].

Nevertheless, Csf1 and Csf1r phenotypes mutant animals, together with PU.1 are the best models to study the trophic roles played by tissue macrophages [24]. The phenotype of the PU.1

knockout is characterized by the depletion of B cells and granulocytes and also a significant decrease in the size of many macrophage populations [24]. The phenotypes found in Csf1 and Csf1r mutant mice are similar, which means that Csf1r is the only receptor for Csf1. However, the severity of some phenotypes is more evident in $Csf1r^{-/-}$ mice, which rarely live beyond a few weeks of age. The phenotypes include complete loss of epidermal Langerhans cells and microglial cells. Conversely, these populations of cells are relatively normal in the $Csf\text{-}1^{op/op}$ mice. This could be explained by the existence of other ligands that could link to the Csf1r, as IL-34, which supports myeloid-cell development in vitro [43].

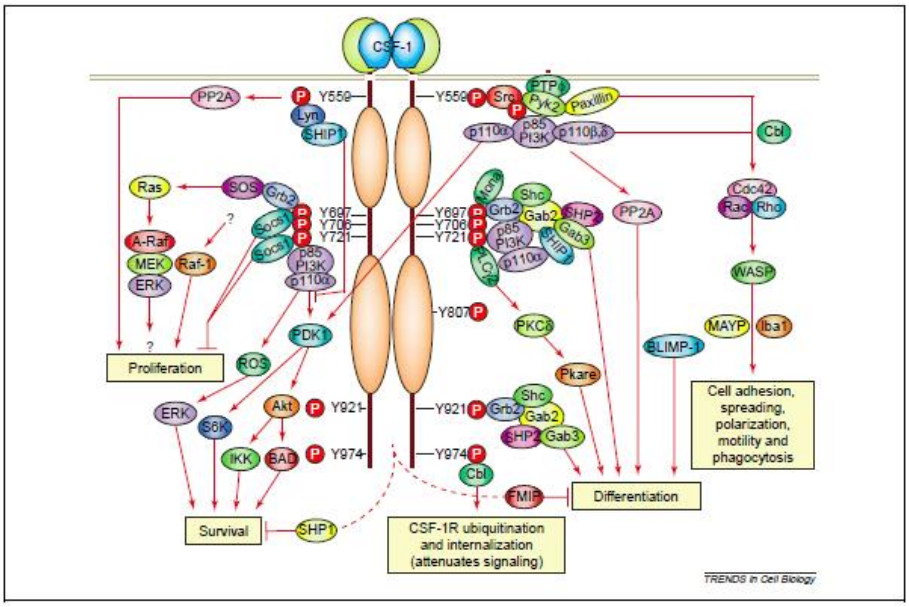

Figure 4. **CSF1/CSF1R Pathway.** Colony-stimulating factor-1 receptor (Csf-1r) activation leads to regulation of different signaling pathways in myeloid cells. CSF1 binding to CSF-1R kinase triggered its tyrosine phosphorylation and generate the activation of signaling molecules associated with the receptor through their phosphotyrosine-binding domains [36].

1.2.3. Macrophages subsets

Macrophages display functional plasticity, which allows their polarization in a diversity of subsets (**figure 5)**. The microbial and cytokine environment drives macrophages to express specialized and polarized functional properties allowing their wide functional heterogeneity [44]. Several macrophages subsets with distinct functions have been described.

Macrophage activation can be either pro-inflammatory or anti-inflammatory leading to tissue damage or renewal and wound healing [45]. Classically activated macrophages, designated as M1, mediate defense of the host from intracellular pathogens, being activated by lipopolysaccharide and interferon- γ. These macrophages are commonly characterized by interleukin (IL)–12^{high}, IL-23^{high} and IL-10^{low} phenotype. They express pro-inflammatory cytokines

such as IL-12, IL-23, IL-1beta, IL-15, IL-18 and TNFalpha, which are involved in the T helper 1 (TH1)-cell-mediated immune resolution of infection. They also produce chemokines and abundant amounts of reactive oxygen and nitrogen intermediates [44, 45]. Functionally, M1 cells enhance endocytic functions and improve the capacity to kill intracellular parasites [46, 47]. Alternatively activated macrophages, defined as M2, have anti-inflammatory function, enhance debris scavenging, angiogenesis, wound healing, tissue remodeling and repair [24]. They are involved in processes such as extracellular matrix (ECM) production and release of trophic factors. M2 cells have been described in a number of variants, depending upon the stimuli used to generate them. These cells generally share an IL-12^{low}, IL-23^{low}, IL-10^{high} phenotype; have high levels of scavenger, mannose and galactose-type receptors. They ensure the production of ornithine and polyamines through the arginase pathway and are IL-1 receptor antagonist (IL-1ra) ^{high}, IL-1decoyR ^{high}, IL-1b^{low} and caspase1^{low} [48]. They can be subdivided in M2a, stimulated by type II cytokines IL-4 or IL-13; M2b, obtained by triggering of Fcgamma receptors in the presence of a Toll receptor stimulus; and M2c which includes deactivation programs elicited by GC, IL-10 or TGFbeta [45]. The different types of macrophages are specified by the microenvironment, although there is considerable plasticity between distinct types. These two distinct profiles show that the macrophage activation can be either pro-inflammatory or anti-inflammatory, contributing to tissue destruction or regeneration. The diverse macrophages functionality has contributed to demonstrate their tissue trophic role namely through their implication in pathology [49].

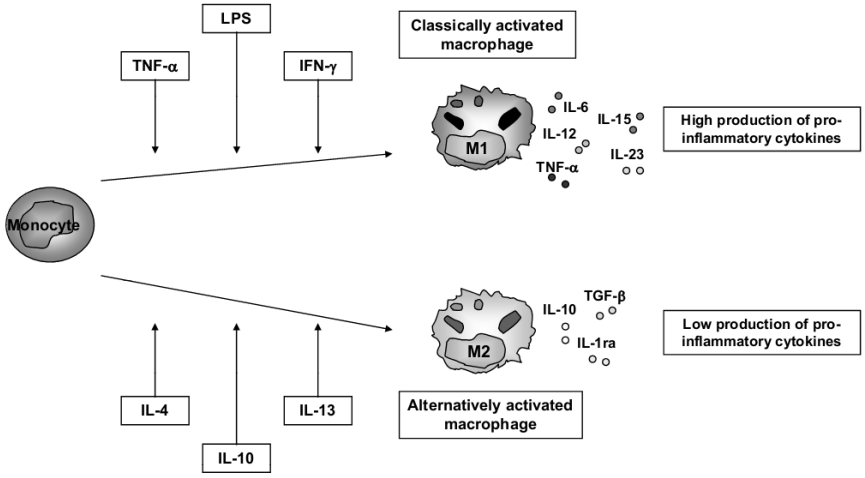

Figure 5. Macrophage activation and polarization. Within the tissue, monocytes can polarize in M1-type, classically activated macrophages, when it's exposed to pro-inflammatory cytokines such as TNF-α and IFN- γ or LPS. And these macrophage populations are characterized by high production of pro-inflammatory cytokines such as TNF-, IL-6, IL-12, IL-15 and IL-23. On the other hand, when monocytes are stimulated by IL-4, IL-13 or IL-10, they generate alternative activated macrophages (M2-type), which produce low levels of pro-inflammatory markers and high levels of anti-inflammatory mediators such as IL-10, IL1ra and TGF- β[50].

1.2.4. Relevance of Tissue Macrophages

In mammals, macrophages are found throughout the body tissues (**figure 6**). They are strategically located to answer inflammatory conditions, being able to ingest and process external materials, dead cells and debris and call for additional macrophages [24].

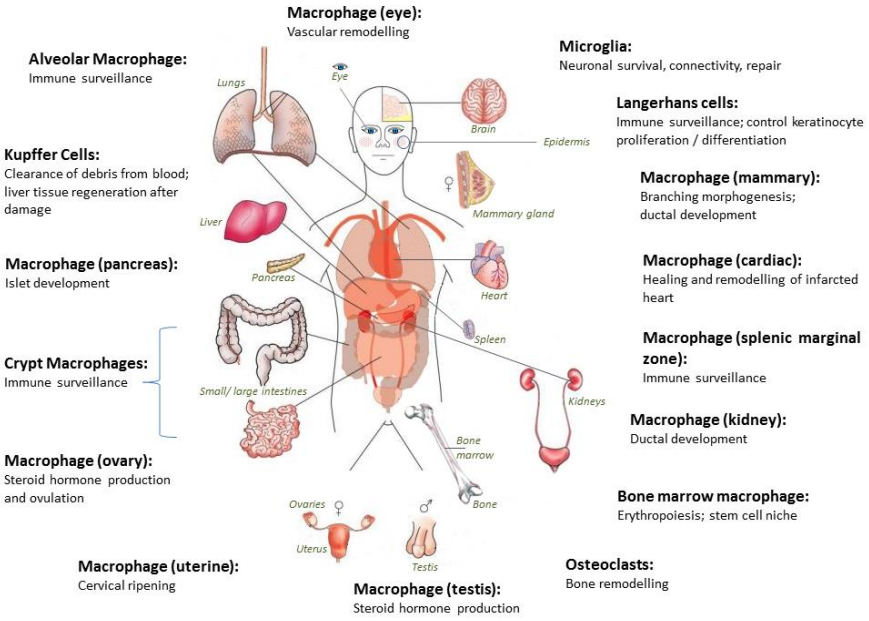

Figure 6. Distribution of body tissue macrophages. Macrophage precursors are released into the circulation as monocytes and then migrate into all body tissues, differentiating into mature macrophages. They are strategically located throughout the body where they have specialized functions [51].

Based on their anatomical localization and functional phenotype, macrophages are divided into subpopulations of mature tissue macrophages [24, 49]. Tissue-resident macrophages comprise osteoclasts (bone), alveolar macrophages (lung), histiocytes (interstitial connective tissue), Kupffer cells (liver), among others[49]. The levels of macrophages in these tissues are variable. For instance in microglial cells in the brain and Kupffer cells in the liver they constitute 10–20% of all cells , but in other tissues their levels are low, such as at the musculo–skeletal junctions [52, 53]. Besides the recognized function of macrophages in disorders induced by pathogens, it is being increasingly accepted that they also have unique non-pathogen induced functions in tissue homeostasis, remodeling and reorganization. Higher levels of macrophages are present in almost all developing organs, with a spike correlated with key periods of organogenesis [54]. Among other functions, macrophages are crucial in processes such as branching morphogenesis, neural patterning, angiogenesis, bone morphogenesis and the generation of

adipose tissue [24]. They are fundamental in the normal development of several organs, as the mammary gland, pancreas and kidney, and the development of these organs is mainly characterized by branching morphogenesis, which is decisive during lung organogenesis [31, 55, 56]. In all these cases, the macrophage depletion leads to tissue impairment formation, responsible by their inadequate function.

1.2.4.1. Bone morphogenesis

Analysis of spontaneous mouse mutants or mice with experimental gene disruptions has highlighted key steps in the differentiation and activation of osteoclasts. Specifically, the use of CSF-1$^{op/op}$ mice determined that the ablation of CSF1 results in a defective development of a common monocyte-osteoclast bone marrow progenitor cell. This progenitor cell under the stimulus of the receptor activator of nuclear factor-kB ligand (RANKL) becomes a multi-nucleated functional osteoclast (**figure 7**)[57].

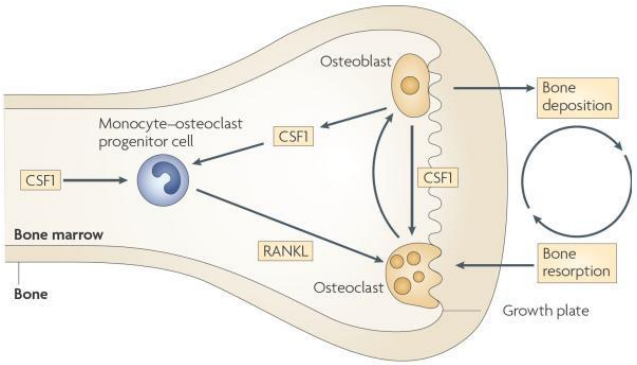

Figure 7. The trophic role of macrophages in bone morphogenesis. The formation of monocyte- osteoclast progenitor is dependent of Colony stimulating factor 1 (CSF1) in the bone marrow that then proliferates and differentiates in the presence of receptor activator of nuclear factor-κB ligand (RANKL) give arise to multinuclear osteoclasts[24].

The most striking phenotype of CSF-1$^{op/op}$ mice is osteopetrosis, with skeletal abnormalities and tooth eruption failure due to osteoclasts depletion. This phenotype is also common in Csf1$^{-/-}$ rats (known as toothless rats; *tl* rats) and PU.1-deficient mice that reveal early myeloid defects and an impaired development of both macrophages and osteoclasts [42, 58, 59]. CSF1 is also responsible to enhance mature osteoclastic bone reabsorption [60]. Remodeling of bone occurs throughout adult life and is controlled by the interaction of bone marrow stromal cells/osteoblasts and osteoclasts. Without functional osteoclasts, the normal re-sculpted of bone doesn't happen, leading to osteopetrosis. Osteopetrosis causes the fail in the marrow cavity

orchestration, which leads to ablation of the most part of haematopoiesis that normally occurs in the bone marrow, although still occurs extramedullary hematopoiesis in the liver and spleen [61]. Csf1$^{op/op}$ mice also show the absence of teeth because the tooth buds, although formed, cannot erupt through the jaw [42, 59]. This osteopetrotic phenotype is one of the best examples of the irreplaceable function of specialized macrophages and their tissue-trophic role.

1.2.4.2. Mammary gland development

Macrophages are an important component of the mammary gland stroma and the ablation of this cell population results in defective ductal elongation, decreases fibroblast growth factor (FGF)-induced mammary epithelial proliferation, suggesting their direct or indirect actuation in mammary epithelial proliferation [62, 63]. This fact could be explained because several cell types, including epithelial, fibroblasts, adipocytes and endothelial cells, composing the mammary gland, and macrophages are known to interact [55]. In mice, the initial mammary ducts give place to multilaminate bulbous termini called terminal end buds (TEBs) [24]. At the same time that TEBs begin to grow during puberty, macrophages are recruited and align along the neck of the TEB structures and their presence is critical for proper ductal elongation (**figure 8**).

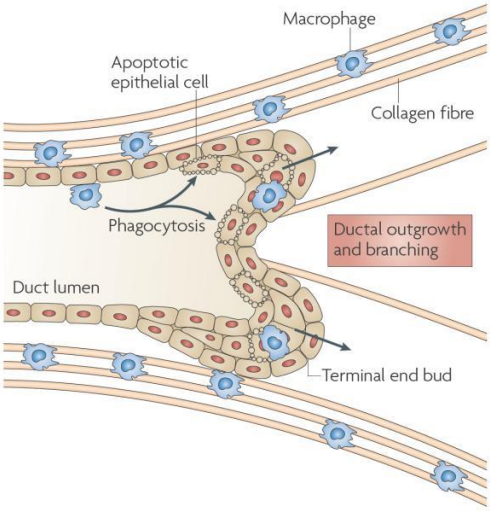

Figure 8. The trophic role of macrophages in ductal branching. Macrophages are associated with epithelial structures including terminal end buds (TEBs) and are often associated with collagen fibres, which they help to form. Loss of macrophages results in defective ductal elongation and disrupts collagen fibrogenesis [24].

Studies in CSF-1$^{op/op}$ mice demonstrated the correlation between macrophages action and mammary development. These mice showed a decrease in ductal elongation associated with the fact that macrophages were not recruited to the TEB structures and the rate of outgrowth of these structures and their branching was decreased [64]. On the other hand, the cross of these

mice to transgenic mice overexpressing CSF-1 under the control of the mouse mammary tumor virus (MMTV) promoter overcame the atrophic mammary gland, meaning that this effect is due to local production of CSF-1 rather than a systemic effect [65]. Although the mechanism of macrophage activity remains not fully understood, the formation of collagen fibrils but not collagen I synthesis is inhibited in CSF-1$^{op/op}$ mice. The restoration of macrophage activity results in the formation of normal fibrils and normal ductal outgrowth and branching, being evident the relevance of macrophage in matrix remodeling of mammary gland [66]. It is accepted that different populations of macrophages may exist in mammary gland and these populations may reside at different levels of M1/M2 with actions dictated by external stimuli.

1.2.4.3. Neural networking/Reproductive system

Macrophages are found throughout reproductive tissues [67]. In this way, one of the approaches to determine their role, using CSF-1$^{op/op}$ mice, shows severe defects in the reproductive system. One of the implications is associated gonadal tissue. In male mice, macrophages are closely associated with testosterone- producing Leydig cells in the testis, and their ablation using a liposome encapsulated clodronate suppress testosterone synthesis. Female mice shows poor ovulation rates, since that macrophages are recruited to the interstitium of the developing ovarian follicle, and the maximum number of these cells is present before ovulation. Nevertheless, analyses of CSF-1 nullizygous mice suggest that the primary reproductive defect occurs in the regulation of the hypothalamic-pituitary-gonadal axis [24]. In male mice, the concentration of circulating luteinizing hormone (LH), which is the pituitary hormone responsible for testosterone biosynthesis, is reduced by 90% compared to control mice [68]. To determine whether this was due to a primary defect in the pituitary, CSF-1$^{op/op}$ mice were treated with the GnRH agonist, histrelin, and the levels of circulating LH were rescued [68]. These data suggest that CSF-1$^{op/op}$ male mice have a primary defect in their hypothalamic axis. In female, there is also decreased negative feedback response to oestrogen removal and a full absence of the positive feedback to oestrogen that causes the surge in LH, resulting in impairment of the ovulation [24]. These evidences are consistent with the relevance of macrophages during the development and maintenance of reproductive system and neural networking.

1.2.4.4. Brain

In the brain the number of macrophages is large, known as microglial cells, which represent around 15 % of total value of brain cells. These cells seem to be the only ones that express CSF1R in the brain during development and in adult-hood [53, 69]. The brain of CSF-1$^{op/op}$ mice is grossly normal, with unremarkable cytoarchitecture, and microglia appear to be normal in the adult, but these animals shows a small development delay in their acquisition [70, 71]. On the other hand, in CSF1r$^{-/-}$ mice there is a complete absence of microglia population, resulting in strong defects in brain such as swollen ventricles, thinned cortex and decrease in olfactory bulbs[72]. This different phenotype could be explained by the IL-34 action, acting as an alternative ligand for CSF1R. In vitro studies of rat embryonic brains, the CSF1 treatment induced outgrowth and neuronal survival in mixed cultures but not in pure neuronal cultures [73]. Although the precise molecular base of microglial cells in brain remains unknown, it is instructive the relevance during wound repair orchestration after brain injury [74]. For instance, in paraplegic rats the macrophage implantation is followed by a regeneration of spinal cord, and in ischemia model the selective ablation of microglial cells exacerbates ischemic injury in the brain [75]. Microglial cells have been recognized to produce growth factors, such as insulin-like growth factor 1 (IGF1), neurotrophic and protective factors [24]. These data shows the relevance of macrophages in the establishment of neuronal circuitry during development.

1.2.4.5. Angiogenesis

Macrophages have been recognized as important players of angiogenesis during wound healing, producing a variety of factors that can regulate vascular potential [24]. However, only more recently their relevance in developmental angiogenesis has been explored. During eye development, the role of macrophage in vascular remodeling was showed. Macrophage ablation, either using a suicide gene approach or through their loss in PU.1-deficient mice, results in a failure of remodeling and persistence of the eye vascular deficient structure post-natally [76]. The mechanism of macrophage action is through their production of WNT7B, which stimulates neighboring vascular endothelial cells to enter the S phase of the cell cycle. More, the action of Ang-2 produced by pericytes leads to endothelial cells undergoes apoptosis to be phagocytosed

by the macrophages (**figure 9**) [77, 78]. Therefore, macrophages allow that the vascular remodeling occurs, and ensures the phagocytosis of apoptotic endothelial cells.

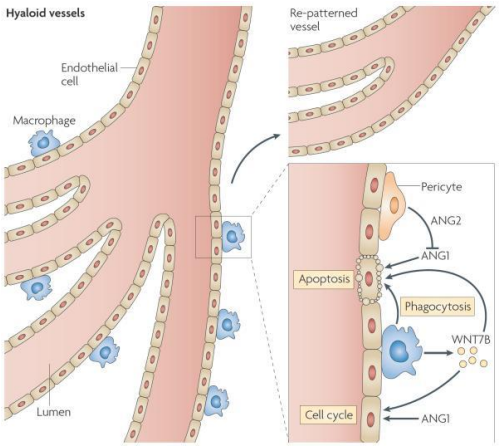

Figure 9. Macrophages interference in angiogenic and vascular eye development. The hyaloid vessel system remodeling is dependent of the vessels synthesize WNT7B, which leads to vascular endothelial cells to enter the DNA synthesis phase of the cell cycle. And the angiopoietin 2 (Ang-2), produced by pericytes blocks the survival signal from Ang-1, which allows that the endothelial cells suffering apoptosis are phagocytosed by the macrophages [24].

In brain development was shown that these cells promote vascular networking and this effect appears as being due to an interaction with endothelial tip cells. This association was observed during all phases of vascular networking formation. Also it was showed that yolk sac–derived macrophages colonized the embryonic mouse brain independently of vessels, as previously reported for the chick macrophages accumulated in the subventricular zone (SZ) between E 10.0 and E 11.5. From this moment, the vessels began to sprout laterally and fused with neighboring vessel branches to form the subventricular vascular plexus. Furthermore, the number of macrophages in the SZ peaked at E 11.5, the major phase of vascular networking. The ablation of macrophages using PU.1-null mice results in hindbrains with significant reduction in the number of vessel intersections and thereby decreased subventricular vascular plexus (SVP) complexity. Fewer connections also formed between neighboring radial vessels compared with wild-type hindbrains at the time when vascular networking was initiated in deeper brain layers. CSF1- deficient hindbrains had an SVP with reduced complexity, similar to PU.1-null mice [79]. These findings suggest that early tissue macrophages play an essential role in brain angiogenesis.

1.2.4.6. Pancreas

In the primary postnatal pancreas of different mouse strains, mature macrophages have been detected from birth on. The number of F4/80 positive cells significantly decreases from birth to weaning. This fact could be explained by the exocrine expansion associated with the postnatal development of the pancreas, but can also mean the earliest F4/80 fetal macrophages disappearance. Despite the critical influence of macrophages in the development and pathogenesis of diabetogenesis, as a result of their infiltration in intra-islet, they have not been clearly described in noninflamatory conditions. Under physiological conditions, the characterization of macrophage population was performed, and macrophages were first observed in the pancreas at E14.5 and remain present in the fetal pancreas at E17.5. It was also observed the presence of macrophage precursors at E12.5 in the fetal pancreas, pancreatic buds along with stomach and duodenal loops [56]. The F4/80+ cells, observed at E14.5, do not likely enter the pancreas via blood circulation, since that functional blood vessel are not observed until E15.5 in the murine pancreas [80].The association between macrophages and tissue organogenesis was described. In vivo studies demonstrated that macrophage ablation results in abnormal postnatal islet morphogenesis and impaired pancreatic cell proliferation [81]. Pancreatic explants were excised and cultured with or without M-CSF. F4/80+ cells were observed in the explants, for both cases, after 5 days of culture. However, the supplementation with M-CSF induced a significant increase in the number of F4/80+ cells in the explant area. Also, it was examined that the addition of M-CSF, and the consequent increase in macrophage number, increase more than fourfold the number of positive insulin cells (insulin- and glucagon-expressing cells) in the cultured explants. Possibly, this effect is mediated via differentiation and activation of the macrophage precursors that were present in the explant [56]. These results allowed concluding an important role in the development of fetal pancreas macrophages.

1.2.4.7. Kidney

Fetal macrophages are among the first hematopoietic cells found in the kidney, appearing in the renal interstitium between E11.5 and 12. It was demonstrated the co-localization of F4/80 with Csf1r-positive cells in the interstitium surrounding the ureteric bud, using a *Csf1r*-EGFP mice. Their localization appears to be contiguous to the vascular development bed between the metanephric mesenchyme and the metanephric ducts, suggesting that possibly macrophages

enter the renal mesenchyme from or with the circulation. The supplementation with CSF-1 to E11.5-12 kidney explants culture resulted in a significant increase in the number of branch tips and nephrons [31]. Associated with this effect was showed the increase in EGFP-positive cells as a result of an increase in the macrophage population. However, there are several ways to the CSF1 actuation in the kidney development, such as macrophage response with the production of critical factors, as growth signal mediating surface tethered, or transmembrane proteins able to signal to adjacent renal cells. Other effect could be an increase in the clearance of apoptotic cells due to macrophage activation. However, apoptotic markers in the explants are not significant different with or without CSF-1 stimulation. Other possibility is the CSF-1 effect in the number of resident macrophages, which increases the proliferative environment. Finally, CSF-1 could directly signalize to another cell population within the kidney. Rather than an immunological role assigned to macrophages, these findings suggest a trophic role during embryonic kidney development [31]. During post-natal development, a similar approach was used to identify the relevance of macrophages in postnatal organ growth and kidney repair. CSF-1 administration to newborn mice increased overall body weight and kidney weight and volume. Moreover, using Csf1r-reporter mouse it was showed that this effect was accompanied by an increase in macrophage numbers in the kidneys.

1.2.5. Lung macrophages and inflammatory mediators in lung development

1.2.5.1. Lung macrophages

The adult lung macrophage population could be subdivided in two principal types: alveolar and interstitial macrophages, localized in separate anatomical compartments in the lung, including the air spaces and lung connective tissue, respectively [82, 83]. Alveolar macrophages are localized within the alveolus, strategically located to answer as primary defense of the lung against inhaled particles [84, 85]. Interstitial macrophages are closely associated with matrix and connective-tissue of lung, representing around 40% of the total macrophages in lung tissue [86]. Interstitial macrophage exhibits a power greater than alveolar to proliferative and this capacity is possible related with the maintenance of lung macrophage pool [40].

During mice lung development, macrophages are found since the begining of development around E10, and remains during throughout development [87, 88].

Immunofluorescence labeling to F4/80 macrophage marker in E12.5 embryonic lungs, showed that macrophages are located extensively accumulated within developing lungs, particularly within branch points. At E15.5 the relative abundance of macrophages in lung is around 5% of total cells. More, their characterization shows enrichment in a lot of genes common with tumor associated macrophages (TAM), suggesting similarities between fetal and tumor environments [31]. On the other hand, more recent findings showed that macrophages are closely associated with maturation of lung. During the saccular stage at post-natal day (P) 1 and P 5, around 8% of total lung cells are macrophages. The increase of these cells is greater during postnatal development, particularly, during alveolarisation, from P 14-21 approaching the 16%, and at 3 months a significant resident macrophage population is maintained. More, during alveolarization it was showed the upregulation of Arginase 1 (Arg1), mannose receptor 1 (Mrc1) and chemokine C-C motif ligand 17 (Ccl17), a phenotype of an M2 or tissue remodeling macrophages [88]. These facts shows that macrophages are present during all lung development but their levels are variable. Despite the deep characterization of macrophage population during post-natal periods and to lesser extent during fetal development, the real contribution of macrophages to lung development remains unknown.

1.2.5.2. Cytokines as mediators in lung development

Some cytokines commonly secreted or regulated by macrophages have been demonstrated to modulate fetal lung branching and maturation [89, 90]. Besides their crucial role in inflammation and the immune response, some cytokines are important players in hematopoiesis, liver and neuronal regeneration, embryonic development and fertility. Their action is mediated by the activation of target genes involved in crucial processes of development such as differentiation, survival, apoptosis and proliferation [89]. During lung development, the relevance of some cytokines has been described. For instance, IL-6 is constitutively expressed in rat pulmonary primitive epithelium, displaying highest levels during earliest stages, which decrease during the following stages of development. Also LIF is important during lung development. Although Leukemia inhibitory factor (LIF) knockout mice have normal lung formation, it is known that LIF, together with insulin-like growth factor I (IGF-I), regulates lung maturation. LIF in addition to IGF-I null mutant mice aggravates pulmonary immaturity, namely LIF/IGF-I double deficient embryos show lung hypoplasia and defective differentiation of the

alveolar epithelium and vasculogenesis. Likewise, TGFβ is expressed at high levels during normal lung development, being crucial for branching morphogenesis and epithelial cell differentiation with maturation of surfactant synthesis [91]. Other cytokine associated with lung development is TNF-a receptor found throughout the embryonic lung and the supplementation with TNF-a in vitro of embryonic lung primordial have a stimulatory effect on branching morphogenesis and surfactant-associated protein (SP-A) expression [92].

Concerning lung maturation, the overexpression of pro-inflammatory mediators, for instance TNF-α, transforming growth factor α (TGF-α), IL-11, or IL-6, in mice lungs results in pathologic situations leading to impairment in alveolarization. The overexpression of the enumerated factors results in fewer and larger alveoli and fibrosis. [93]. The previous data suggests that lung development is highly regulated by cytokine environmental. Being macrophages relevant players in cytokines expression, their possible relevance during lung development is overwhelming.

1.10 Rationale and Aims

Besides their function during the development in other organs, macrophage function during lung development remains unknown. Therefore, this master thesis aims to understand the relevance of tissue macrophage ablation during lung development. Tacking in account that disruption of *Csf1r* gene results in large depletions of macrophages in most tissues, in order to accomplish this aim, we perform a characterization of lung development using a macrophage-deficient mouse model ($Csf1r^{-/-}$). Three specifics points of lung development were evaluated: the pseudoglandular (at E15.5), the fetal saccular stage (E18.5) and the post-natal saccular stage (P0). For all stages tree groups/genotypes $Csf1^{+/+}$ $Csf1r^{-/+}$ and $Csf1r^{-/-}$ were compared:

- At pseudoglandular stage it was performed the evaluation of gross morphology, bud number quantification and lung morphology characterization, in which stereological analyses was used. For the last evaluation it was used stereological analysis. Specifically, it was measured epithelial, mesenchymal and air space volume density (VD). Additionally, it was performed evaluation of lung vasculature: vessel density quantification using the endothelial cell marker CD31 (PECAM-1), by immunohistochemistry. Beyond this, assessment of transcripts expression patterns of angiogenic factors and associated molecules (such as VEGF-A, VEGFR2, Ang-1, Ang-2, Hif1α and Fgf2) was performed by q-RT-PCR.

- At the fetal saccular stage (E18.5) it was also evaluated lung morphology by the same parameters described. Concerning lung vasculature, beyond the parameters evaluated at E15.5 stage, it was evaluated the artery thickness, using Weigert's staining.

- At post-natal saccular stage (P0), beyond the previous lung morphology evaluation at E15.5 and E18.5, lung-to-body weight ratios were accessed. Regarding, stereological analysis, beyond the mesenchymal, epithelial and air space volume, it was also evaluated the large and small airway epithelium VD. Blood gasometrical evaluation was performed as readout of lung functionality. Regarding lung vasculature all parameters evaluated at E18.5 stage were also evaluated.

MATERIALS AND METHODS

2. MATERIALS AND METHODS

2.1. Animals

All procedures and protocols were carried out in accordance with European Union Directive 86/609/EEC and NIH guidelines on animal care and experimentation. Mice of mixed genetic background (C3H/C57BL/6) and deficient in Csf1r ($Csf1r^{-/-}$) were kindly provided by Prof. E. Richard Stanley, Albert Einstein College of Medicine University Yeshiva, Bronx, USA. Animals were fed ad libitum and exposed to day-night cycles alternatively every 12h.

2.2. Study design

The $Csf1r^{+/-}$ animals were crossed and the vaginal plug checked 12 hours after and defined as embryonic gestational day 0.5 (E0.5). At E15.5 and E18.5 stages, dam were sacrificed by cervical dislocation, embryos were removed by caesarean section. Embryos and newborns (post-natal day (P) 0) were sacrificed by decapitation and lung excised under stereomicroscope (Olympus SZX7). Depending on the analysis required, different lung tissue processing was performed. To evaluate mice genotype, a small piece of tissue of each animal was collected. The tree different embryos/newborns genotypes were assessed using PCR analyses. Then, the animals were subdivided into 3 groups: $Csf1r^{+/+}$ (wild type or control); $Csf1r^{+/-}$ and $Csf1r^{-/-}$.

2.3. PCR analyses for Genotyping

Pellet was diluted in ultrapure H_2O and let to dissolve overnight. Detection of CSF1R transgene was done using a primer specific to a fragment Csf1r. Genomic DNA was extracted from tissue pieces and incubated overnight at 55° in lysis buffer (100 mM TRIS (pH8), 0.2 % sodium dodecyl sulfate (SDS), 5mM EDTA) and proteinase K (85μg/ml). After centrifuged 10 min at 14000g, isopropanol was added to the supernatants collected, centrifuged 5 min at 14000g, the new supernatant discarded and pellet dried by incubation at RT. Pellet was diluted in ultrapure H_2O and let to dissolve overnight. Detection of Csf1r transgene was done using a set of specific primers to a fragment Csf1r. The final concentrations in the PCR reactions were: 50ng of extracted DNA, 200 μM of each dNTP, 1.5mM MgCl2, 1.25 U *Taq* DNA Polymerase (Promega) and 0.4 μM of each primers (Csf1r-Intron 2 Forward: 5'AGACTCATTCGAACCAGAGAGC-3'; Csf1r-

InEx 3 Reverse: 5'-GAATTTGGAGTCCTCACCTTTG -3'; Csf1R-Neo-Forward: 5' CCGGTAGAATTCCTCGAGTCTA-3'). Amplification (Mycycler™thermalcycler, BIO-RAD) was performed as follows: 92° for 20 sec (initial strand separation); 35 cycles of 94° (20 sec), 58° (45 sec) and 72° (1 min); and 72° for 7 min (final elongation step). The PCR fragment size expected to presence of Csf1r gene (wild type animals) was 385 bp and to absence ($Csf1r^{-/-}$) was 308 bp. These were visualized by electrophoresis in 4% agarose gels.

2.4. Lung-to-body weight ratios

After birth (P0), newborn were killed by decapitation and lung excised under a stereomicroscope. The right and left lungs and the entire animal were weighed independently and lung-to-body weight ratios were assessed. The evaluation was performed to the tree genotypes ($Csf1r^{+/+}$: n=8; $Csf1r^{-/+}$: n=11 and $Csf1r^{-/-}$: n=4).

2.5. Neonatal blood gasometric evaluation

The newborn were killed by decapitation and the blood collected (neck bleeding) to perform gasometric evaluation. The parameters calculated were: pH, PCO_2 (Partial Pressure) (mmHg), PO2 (mmHg), $SatO_2$ (Saturation) (%) and Lactate (mmol/L) using a gasometric analyser (i- Stat1 analyser; Abbott, Chicago, IL, USA). The evaluation was performed for the tree genotypes at P0 stage ($Csf1r^{+/+}$: n=4; $Csf1r^{-/+}$: n=5 and $Csf1r^{-/-}$: n=2).

2.6. Stereological Analyze

To stereological analyses, the trachea was cannulated and the lungs were insufflated with fixation solution (glutaraldehyde 2,5% in PBS) under a constant pressure of 1 rpm during 1 min using a peristaltic pump (Gilson, Model Minipul S3). The lungs were dissected and kept in fixation solution on agitation, until its processing. Briefly, the lungs were dehydrated in increasing concentrations of ethanol and xylol, embedded in methacrylate, consecutively cut in slides with 15 μm and stained with hematoxylin-amoniacal. Stereological analysis was carried out by one person, blinded to the genotype of the animal, on a Zeiss microscope Axioplan 2 (Tokyo, Japan) using the Stereo Investigator version 5.2 software (MicroBrightField). A fixed range of 30 to 30

slides per animal was used; the 15µm-thick hematoxylin stained slides from each animal were analyzed using a grid of test points. The total number of points and intersections in each lung were >1,000. Morphometric parameters, such as total, mesenchymal, epithelial, air space, alveolar and bronchiolar lung tissue volume were calculated according to the point and intersection counting. Briefly, all points (intersections) which laid over a point count were counted and were represented as a proportion of total points. The volumes were calculate by the Cavalieri principle $VL = h \cdot \sum P(sl) \cdot d^2$ (h- thickness, sl-point number, d-distance between grid points) [94]. The percentage of volume density relative to all lung tissue was calculated for $Csf1r^{+/+}$, $Csf1r^{-/+}$ and $Csf1r^{-/-}$ animals (n=4, n=5 and n=4 lungs were analyzed at E15.5; n=4, n=4 and n=4 at E18.5; and n=4 n=5 and n=4 at P0, respectively).

2.7. Immunohistochemistry

To immunohistochemical studies the trachea was cannulated and the lungs were insufflated with fixation solution (paraformaldehyde (PAF) 4% in PBS) without pressure control. Then, lungs were dissecated and fixated overnight at RT with agitation. Afterwards lungs were dehydrated in increasing concentrations of ethanol and xylol, embedded in paraffin and 3 µm slides were used. Briefly, paraffin slides were deparaffinized and rehydrated. Antigen retrieval trials were performed in: 10mM of citrate buffer pH=6.0 in microwave or water-bath at 100°C, by 15 and 20 min, respectively. To inactivate endogenous peroxidases, slides were incubated in 3% hydrogen peroxide in MeOH for 10 min. Then, slides were incubated with Avidin/ Biotin for 15 min each and after with normal horse serum (HNS) (VECTASTAIN Elite ABC Kit) for 30 min, followed by an overnight incubation in diluted primary antibody PECAM-1/CD31 (Santa Cruz) in a 1:200 dilution. After, slides were incubated with biotinylated horse anti-goat secondary antibody (Vector Labs) in a 1:500 dilution in HNS for 1h, and next, peroxidase-labeled reagent for 5 min (*VECTASTAIN® ABC reagent, Vector Labs*). Slides were incubated with 3,3'-diamino-benzidine (DAB + Substrate System, DakoCytomation). Finally, slides were counterstained with hematoxylin and permanently mounted. All dilutions were made in PBS, pH 7.5, and all incubations were performed in humid chambers at room temperature. Between each step in the staining procedure (except before incubation with primary antibody), the slides were rinsed twice in PBS. In all reactions a negative control was included, where the staining was performed with the same protocol above described without primary antibody.

2.8. Vessel Density quantification

For evaluation of vessel density, slides were scanned in the light microscope (Olympus BX61, Tokyo, Japan) at × 20 magnification at least in 5 different representative fields of the slide. Vessel density was determined by counting the number of CD31+ vessels per measurement field at × 200 magnification (× 20 lens, × 10 ocular, measurement field of 0.143642mm^2) by a blinded examiner. A vessel was defined as any distinct CD31+ cell cluster with an area exceeding 5 µm^2. The numbers of vessel counted in the analyzed areas were averaged per number cross sections and denoted Vessel Density. The evaluation was performed to the tree groups at E15.5 (Csf1r$^{+/+}$: n=6; Csf1r$^{-/+}$: n=5 and Csf1r$^{-/-}$: n=3), E18.5 (Csf1r$^{+/+}$: n=5; Csf1r$^{-/+}$: n=6 and Csf1r$^{-/-}$: n=3) and P0 stage (Csf1r$^{+/+}$: n=6; Csf1r$^{-/+}$: n=5 and Csf1r$^{-/-}$: n=6).

2.9. RNA extraction and cDNA synthesis

The lungs were dissected and placed immediately in liquid nitrogen and then frozen at -80°C until the extraction. Total RNA from lung samples was extracted using TRIzol® 143 Reagent (Invitrogen, San Diego, CA) with PureLink ™ RNA Mini Kit, according to the manufacturer's instructions. The lungs was kept in ice and added 500, 750 or 1000 µl of TRIzol to E15.5, E18.5 and P0 lungs, respectively. To disrupt the lung sample was used up-and-down movements with a pestle. After lysis, the lysate was homogenized trough an 18 and 25-gauge needle attached to an RNase-free syringe. The lysate was incubated at room temperature for 5 min to allow the complete dissociation of nucleoprotein complexes. Then, it was added 0,2 ml chloform per 1ml TRIzol reagent used, shaking the tube vigorously by hand for 15 seconds, followed by incubation for 2-3 min at RT. The samples were centrifuged at 12,000 x g for 15 min at 4°C and 400 µl of the colorless, upper phase containing the RNA was transferred to a fresh Rnase-free tube, added an equal volume 70% ethanol the tube mixed well, using a vortex. The sample were transferred to a spin cartridge (with a collection tube), centrifuged at 12,000 x g for 15 sec at RT. The flow-through was discarded and this process was repeated until the entire sample was processed. After, the On-column PureLink ™ DNase treatment and purification kit was used to perform the DNA genomic elimination. Then, 350 µl Wash buffer I was added to the spin cartridge containing the bound RNA and centrifuged at 12,000 x g for 15 sec at RT. The flow-through was discarded and the spin cartridge inserted into a new collection tube. 80 µl of

PureLink ™ Dnase mixture was added directly onto the surface of the spin cartridge membrane, incubating at RT for 15 min. 350 µl of wash buffer I was added to the spin cartridge and centrifuged at 12,000 x g for 15 seconds at RT. The flow-through and collected tube and insert the spin cartridge into a new collection tube. 500 µl of Wash buffer II with ethanol was added to the spin catridge and centrifuged at 12,000 x g for 15 seconds at RT, discarding the flow-through and repeated the wash with wash buffer I and with buffer II. The spin cartridge was centrifuged for 1 min to dry the membrane with the bound RNA. Finally, 30-50 µl of Rnase-free water was added to the center of the Spin Cartridge and recovery tube and centrifuged for 1 min at RT. The concentration and purity were analyzed using a Nanodrop® Spectrometer.

After total RNA extraction, 1 µg of total RNA/sample was submitted to reverse transcription with Maxima-Reverse Transcriptase (Thermo Scientific) for 10 min at 25°C, 15 min at 50°C and 5 min at 85°C utilizing 50 pmol random hexameric primers/oligo (dT)18 and random hexamer primers on the MyCycler™ thermal cycler (Bio-Rad).

2.10. Quantitative Real-Time PCR (q-PCR)

Relative gene expression of *Vegfa, Flk1, Ang1, Ang2, Hif1α e Fgf2* was assessed using the Maxima Probe/ROX qPCR Master Mix (2X) (Thermo Scientific). For the following genes with sequence ID (enclosed between brackets), commercially available Taqman probes were ordered (Applied Biosystems): *Vegfa* (Mm01281449_m1), *Flk1* (Mm01222421_m1), *Ang1* (Mm00456503_m1), *Ang2* (Mm00545822_m1), *Hif1α* (Mm01283760_m1), *Fgf2* (Mm 00433287_m1) *Gapdh* (Mm99999915_g1). cDNA expression levels were assessed by quantitative real time PCR reaction (2 min 50°C, 5 min 95°C, 40 cycles at 95° C for 15 sec and 60°C for 1 min) using the CFX96™Real-Time System (Bio-Rad). The housekeeping GAPDH gene was used as internal references for normalization and the transcript levels was calculated by using a comparative threshold cycle method and the formula $2^{(-\Delta\Delta_{Ct})}$ (Ct - threshold cycle) [95].

2.11. Weigert's staining

To Weigert's stain, 3 µm slides paraffin-embedded were used. Briefly, paraffin sections were deparaffinized and rehydrated. After, incubated 1h 30min with Weigert's solution (Weigert's

Resorcin Fuchsin, Sigma-Aldrich), following by tree washes with EtOH 100%, 5min with xylol and mounted.

2.12. Arterial thickness evaluation

For evaluation of arterial thickness, slides stained with Weigert's coloration were scanned in the light microscope (Olympus BX61, Tokyo, Japan) at × 40 magnification at least in 5 different representative fields of the slide. Pulmonary arteries were distinguished from pulmonary veins on the basis of the structure. Arteries with clear visible external and internal elastic laminae (which comprise tunica intima, media and adventitia) were analyzed and the distance between these two points was calculated. The evaluation was performed to the tree genotypes at E18.5 ($Csf1r^{+/+}$: n=5; $Csf1r^{-/+}$: n=5 and $Csf1r^{-/-}$: n=) and P0 stage ($Csf1r^{+/+}$: n=6; $Csf1r^{-/+}$: n=5 and $Csf1r^{-/-}$: n=5).

2.13. Statistical Analysis

All experiments were analyzed using Student's t-test (GraphPad Prism 5). Results are expressed as mean ± SEM. Differences were considered statistically significant when $p \leq 0.050$.

3. RESULTS

3.1. Impact of macrophages deletion in pseudoglandular stage of lung development (E15.5)

3.1.1. Lung gross morphology

In order to evaluate if the Csf1r deletion results in a visible disruption in the pseudoglandular developmental stage (E15.5) of murine lungs, the gross morphology was analyzed. The correspondent pictures are represented above (**figure 10**). The knockouts mutant embryos, $Csf1r^{+/-}$ (n=9) and $Csf1r^{-/-}$ (n=4), didn't show gross lung developmental abnormalities when compared with control (n=8). Also no gross differences in size and aspect were found, between the different genotypes.

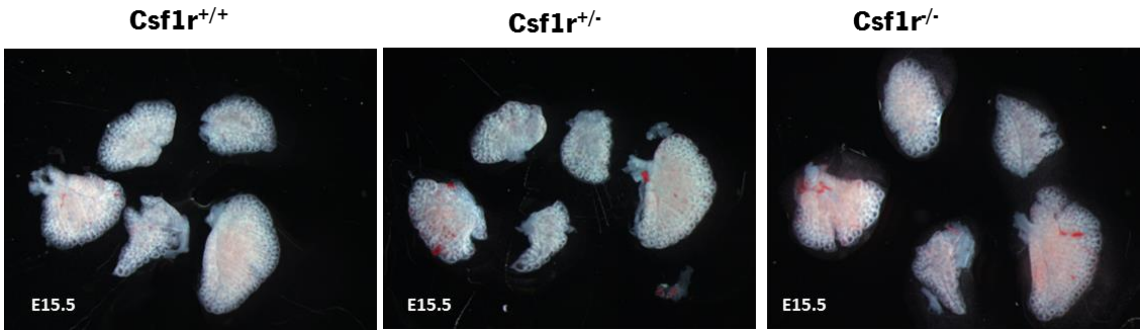

Figure 10. Gross morphology evaluation of lung embryos at E15.5 stage. Above are represented the illustrative lung pictures immediately after dissection at E15.5 stage. No differences in size, shape and gross morphology were found between $Csf1r^{+/-}$ and $Csf1r^{-/-}$ and wild type lungs. Magnification: 1.6x.

3.1.2 Lung bud number

Macrophages are present since early steps of lung development, and closely associated with mesenchyme and with elongating lung buds [88]. In other branching systems, such as kidney, mammary gland and pancreas, macrophages reside in abundant number, providing a strong regulation on organ branching [24]. Therefore, the branching program of lung development could be affect by macrophage ablation. In this way, we evaluated, by gross

dissection at E15.5, if the lungs from knockout mice (Csf1r$^{+/-}$ and Csf1r$^{-/-}$) showed an alteration on lung bud number (**figure 11)**. Indeed, these animals didn't seem to have alteration on branching structures number. In order to check this fact, the number of left lung lobe buds at E15.5 stage was quantified and the results are represented in the **figure 12**.

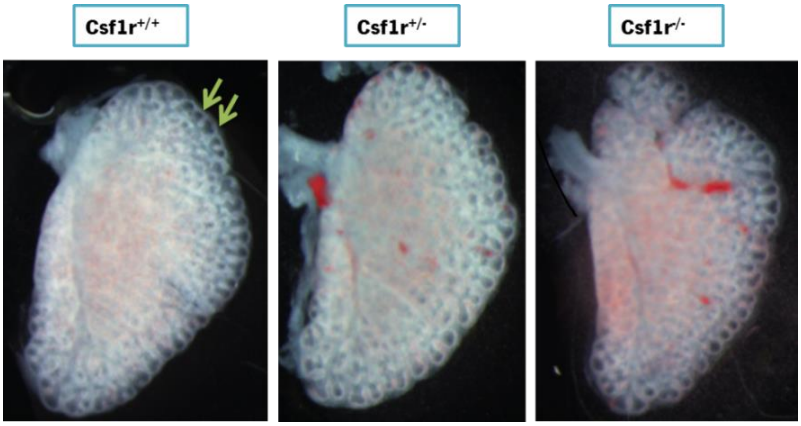

Figure 11. Representative pictures of left lung lobe at E15.5. Above are exemplified the representative left lung lobe pictures immediately after dissection at E15.5 stage. As can be seen the number of buds not appear to be altered in the different genotypes. Arrows indicate bud structures. Magnification: 1.6x.

The Csf1r$^{+/-}$ and Csf1r$^{-/-}$ animals showed a slight decrease in the number of buds, median of 30.07 (n=6) and 30.05 (n=4) respectively, when compared with control group, median of 32 buds (n=2). No statistical significance was found between Csf1r$^{+/+}$ and Csf1r$^{+/-}$ animals (p= 0.729), Csf1r$^{+/+}$ and Csf1r$^{-/-}$ (p=0.788), Csf1r$^{+/-}$ and Csf1r$^{-/-}$ (p=0.949). These results didn't suggest alteration in the branching process for both Csf1r knockouts (Csf1r$^{+/-}$ and Csf1r$^{-/-}$).

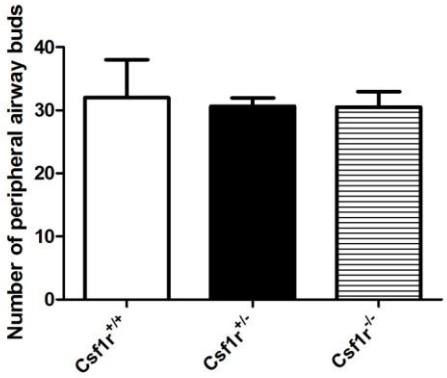

Figure 12. Number of buds in left lung lobe at E15.5 stage. Above are represented the number of buds of left lung lobe of Csf1r$^{+/+}$, Csf1r$^{+/-}$ and Csf1r$^{-/-}$ animals. Both knockout animals, Csf1r$^{+/-}$ and Csf1r$^{-/-}$, show a small decrease in the number of buds of left lobe, without statistical differences. Lungs analyzed: n= 2 of Csf1r$^{+/+}$; n=6 of Csf1r$^{+/-}$; n=4 of Csf1r$^{-/-}$. Data is represented as mean ± SEM.

3.1.3. Lung morphology

In order to characterize the progression of lung formation in the macrophage deficient embryos (Csf1r$^{+/-}$ and Csf1r$^{-/-}$) compared with wild-type (Csf1r$^{+/+}$), the lung morphology was evaluated by stereological analysis of hematoxylin–stained sections. The histological pictures of lung morphogenesis at E15.5 stage are showed below in **figure 13**. No apparent differences in lung morphogenesis were observed in wild-type versus Csf1r$^{+/-}$ embryos. However, when compared the wild type versus Csf1r$^{-/-}$ lung embryos, an increase in mesenchymal and a slight decrease in epithelial and airspace components was observed.

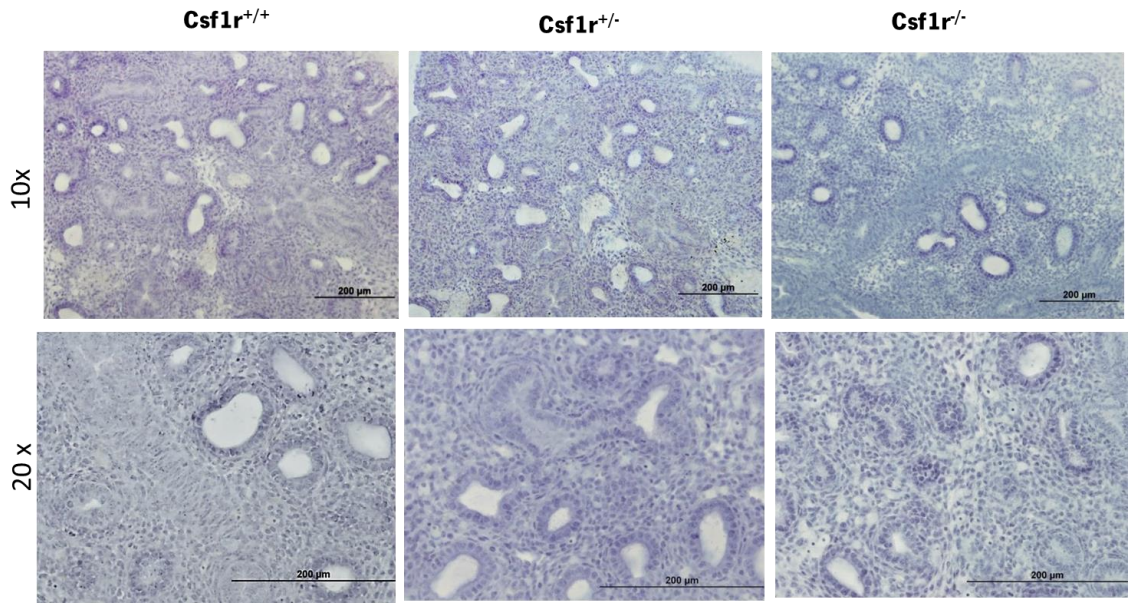

Figure 13. Lung embryos histological sections at E15.5 stage. Representative pictures of lung histology at E15.5 of Csf1r$^{+/+}$, Csf1r$^{+/-}$ and Csf1r$^{-/-}$ animals. An increase in mesenchymal and a decrease in epithelial tissue is observed when compared Csf1r$^{-/-}$ with wild type animals. Magnification: top panel 10 x, bottom panel 20x.

The histologic differences between the different genotype animals were examined in detail, quantifying lung histological structures. Using stereological analyses, the mesenchymal, epithelial and airspace volume density (VD) were determined to Csf1r$^{+/+}$, Csf1r$^{+/-}$ and Csf1r$^{-/-}$ (**figure 14**). Morphometric measurements showed that mesenchymal VD of Csf1r$^{-/-}$ lung embryos presented a 20% increase (67.07±2.22%) compared with wild type embryos (55,96 ±5.45%). However, no statistically differences were found, (p=0.153). The Csf1r$^{+/-}$ group didn't shows remarkable difference (55.56±1.75%) compared with wild type group (p=0.953), but with

significant differences when compared with Csf1r$^{-/-}$ group (p=0.007). Regarding epithelial VD, Csf1r$^{-/-}$ embryos didn't shows significant differences (12.69±0.45%) compared with wild type (13.32±1.40%; p=0.681). Csf1r$^{+/-}$ embryos showed lower values of epithelial VD (10.76±0.43) compared with control (p=0.130) and with Csf1r$^{-/-}$ group (p=0.020). At last, regarding airspace VD, Csf1r$^{-/-}$ lung embryos showed a mean of 3.28±0.28%, Csf1r$^{+/-}$ of 2.60±0.43% and wild type embryos of 3.66±0.37%. No statistical differences were found when compared Csf1r$^{-/-}$ and Csf1r$^{+/-}$ with wild type embryos (p=0.473 and p=0.127, respectively) or with Csf1r$^{+/-}$ (p=0.218).

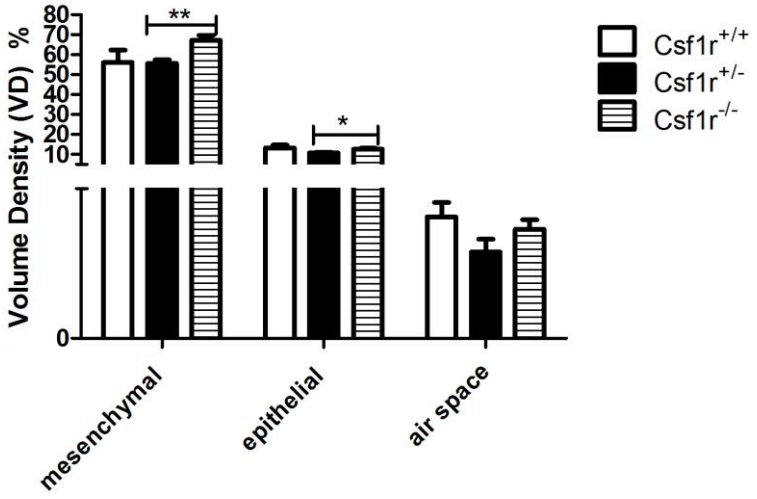

Figure 14. Lung stereological analyses at E15.5 stage. Above are represented the stereological results of mesenchymal, epithelial and air space volume density (VD). Animals analyzed: n=5 Csf1r$^{+/-}$, n= 4 Csf1r$^{-/-}$, n=4 Csf1r$^{+/+}$. The mesenchymal VD was higher in Csf1r$^{-/-}$ lungs when compared with wild type, while epithelial and air space VD were slight decrease. Data is represented as mean ± SEM. *p<0.050;**p<0.010.

1.1.4. Lung vasculature

There is a strong structural and functional association between lung branching and vascular development. The disruption of endothelial cell development is accompanied by an inhibition of airway epithelial cell differentiation and maturation [96]. More, during organ development and remodeling, macrophages support angiogenesis, not only by the expression of proangiogenic factors and matrix-remodeling proteases, but also by the physical interaction with vessels [97]. Thus, we hypothesize that macrophage ablation, trough the Csf1r deletion, may impact lung vascular development. In this way, we assess the lung vessel density using a specific endothelial

cell marker, CD31. At E15.5 stage an apparent increase in the number of CD31 positive vessels were observed in Csf1r$^{+/-}$ and Csf1r$^{-/-}$ compared with wild type (**figure 15**).

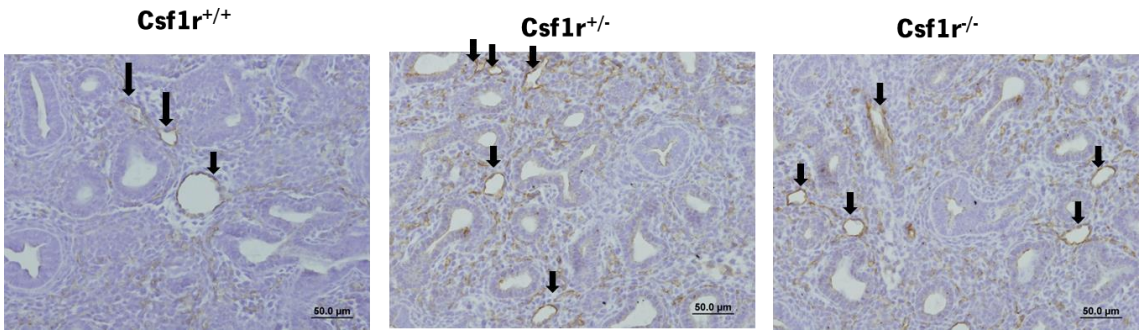

Figure 15. CD31 immunohistochemical staining in lung embryos at E15.5. The CD31 endothelial cell marker was used to stain blood vessels specific cells, endothelial cells (black arrows). An increase in the number of vessels for knockout animals was found at E15.5 stage. Magnification: 20x.

In order to evaluate if the previous subjective analysis of vessel number corresponds to statistical difference in the number of vessels, the vessel density was calculated for the different genotypes. The vessel density was determined by counting CD31 positive vascular structures per lung sections and the results are in **figure 16**. Csf1r$^{+/-}$ showed a vessel median of 4.10±0.38, Csf1r$^{-/-}$ of 4.08±0.55 and wild type of 3.37±0.47. Therefore, knockout animals presented a minor increase in the vessel density compared with control. However, no statistical differences were found (Csf1r$^{+/-}$ vs wild type p=0.269, Csf1r$^{-/-}$ vs wild type p=0.386, and Csf1r$^{+/-}$ vs Csf1r$^{-/-}$ p=0.980).

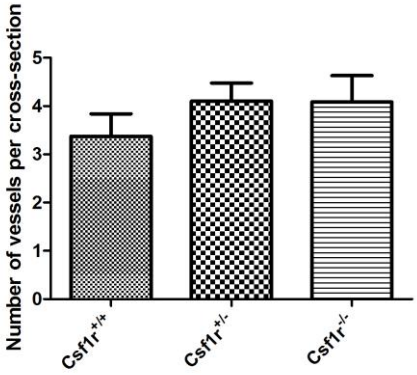

Figure 16. Vessel density in lung embryos at E 15.5 stage. Vessel density was determined by counting CD31 positive vascular structures. Knockout animals (Csf1r$^{+/-}$ and Csf1r$^{-/-}$) showed a minor increase in the number of blood vessels. n= 6 of Csf1r$^{+/+}$; n=5 of Csf1r$^{+/-}$ and n=3 of Csf1r$^{-/-}$ lungs were analyzed. Data is represented as mean ± SEM.

3.1.5. Gene expression of angiogenic factors

The vasculature is a result of a balance of pro and anti-angiogenic factors, which drives the orchestration of vascular network. In this way, the evaluation of gene expression of key angiogenic factors during lung development will allow to identify whether the balance is affected and which factors could be involved. Therefore, in this study, we have performed an RNA levels quantification of some angiogenic factors: VEGF-A, Flk-1, Ang-1, Ang-2, HIF-1a and Fgf2 (**figure 17**).

At E15.5 stage, the vascular endothelial growth factor A (VEGF-A) transcripts of $Csf1r^{+/-}$ lungs showed median folds increase of 1.13±0.087 and, $Csf1r^{-/-}$ of 1.16±0.011 relative to wild type (1.00±0.041). However, these differences weren't statistically significant ($Csf1r^{+/-}$ vs wild type p=0.206; $Csf1r^{-/-}$ vs wild type p=0.126; $Csf1r^{+/-}$ vs $Csf1r^{-/-}$ p=0.826). This trend was also observed in the transcripts levels of VEGF-A receptor, Flk-1 (VEGR-2). $Csf1r^{+/-}$ showed median fold changes of 1.47±0.117, $Csf1r^{-/-}$ of 1.30±0.135 and wild type of 1.00±0.052. $Csf1r^{+/-}$ and $Csf1r^{-/-}$ Flk-1 transcripts were significantly increased comparing with wild type (p=0.003 and p=0.018, respectively). Concerning, angiopoietin-1 (Ang-1) expression levels, $Csf1r^{+/-}$ and $Csf1r^{-/-}$ showed no fold changes comparing with wild type (medians to $Csf1r^{+/-}$ 1.06±0.049, $Csf1r^{-/-}$ 1.06±0.076 and wild-type 1.00±0.046). Therefore, no statistical differences were found ($Csf1r^{+/-}$ vs wild type p=0.381, $Csf1r^{-/-}$ vs wild type p=0.941, $Csf1r^{+/-}$ vs $Csf1r^{-/-}$ p=0.541). On the other hand, the gene expression levels of angiopoietin-2 (Ang-2) were 1.53±0.075 fold increase in $Csf1r^{+/-}$ and 1.47±0.143 in $Csf1r^{-/-}$ comparing with wild-type (1.00±0.074), being these differences statistically significant (p=0.0002 and p=0.008, respectively).

Concerning hypoxia inducible factor 1 alpha (HIF-1a) transcripts levels, no statistical differences were found in the mean fold changes of $Csf1r^{+/-}$ (1.00±0.066, 0.975) and $Csf1r^{-/-}$ (0.98±0.101, 0.885) compared with wild type (1.00±0.078).

At last, Fgf2 gene expression levels were significant 2.55±0.147 fold higher in $Csf1r^{-/-}$ (p=0.003). Regarding $Csf1r^{+/-}$, significant differences were observed comparing with wild type (p=0.006), but no with $Csf1r^{-/-}$ (p=0.257).

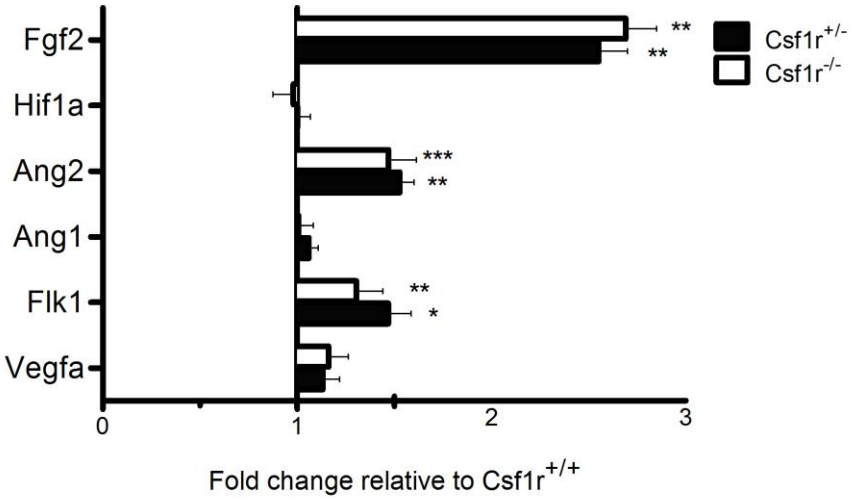

Figure 17. Angiogenic factors gene expression profile by qPCR of lungs at E 15.5. Comparison of VEGF-A, Flk-1, Ang-1, Ang-2, HIF-1a and Fgf2 gene expression of $Csf1r^{+/-}$ and $Csf1r^{-/-}$ with $Csf1r^{+/+}$animals. All genes were normalized against GADPH expression. Lungs analyzed: n= 8 of $Csf1r^{+/+}$; n=9 of $Csf1r^{+/-}$; n=6 of $Csf1r^{-/-}$. *p<0.050;**p<0.010

3.2. Impact of macrophages deletion in fetal saccular stage of lung development (E18.5)

3.2.1. Lung gross morphology

At fetal saccular stage, E18.5, gross morphology observation of $Csf1r^{-/-}$ lungs (n=2) indicated a reduced size when compared with $Csf1r^{+/-}$ (n=4) and wild type lungs (n=6). This difference was particularly pronounced in the left and accessory lobe. However, the shape and lung structure remains unaltered. At this stage, the heterozygotes lungs ($Csf1r^{+/-}$) didn´t appear different in the shape and size when compared with wild type (**figure 18**).

Figure 18. Gross morphology evaluation of lung embryos at E18.5 stage. Above are represented the illustrative lung pictures immediately after dissection at E18.5 stage. At this stage, the Csf1r$^{+/-}$ lungs didn't show apparent difference when compared with Csf1r$^{+/+}$. However, the Csf1r$^{-/-}$ embryos showed smaller lung lobes when compared with wild type and Csf1r$^{+/-}$ lungs. Magnification: 0.8x.

3.2.2. Lung morphology

The lung histology at E18.5 stage is showed below in **figure 19**. No apparent differences in lung morphogenesis were observed in wild type versus Csf1r$^{+/-}$ embryos. However, when comparing wild type versus Csf1r$^{-/-}$ lung embryos an increase in mesenchymal and a reduction in area space tissue were observed. Also, reduction of primitive pre-alveoli (black arrows) in Csf1r$^{-/-}$ were founded compared to wild type lung embryos. These histological analyze showed that the morphogenesis of Csf1r$^{-/-}$ lungs appeared to be delayed at more early stage of development.

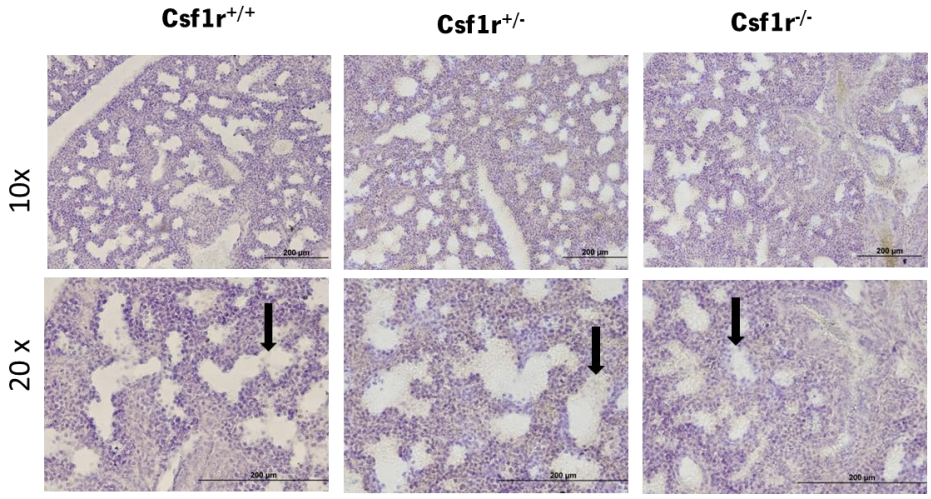

Figure 19. Lung embryos histology at E18.5 stage. Representative pictures of lung histology at E18.5 of Csf1r$^{+/+}$, Csf1r$^{+/-}$ and Csf1r$^{-/-}$ animals. A decrease in epithelial tissue is observed when compared Csf1r$^{+/-}$ and Csf1r$^{-/-}$ with wild type embryos, as well as a reduction of primitive pre-alveoli (black arrows). The Csf1r$^{-/-}$ animals showed also an increase in mesenchymal tissue compared with wild type group. Magnification: top panel 10 x, bottom panel 20x.

In order to quantify these observations, stereological analyses were performed. Morphometric measurements (**figure 20**) showed that mesenchymal VD of Csf1r$^{-/-}$ lung embryos were significantly higher (14.66±1.17%) compared with wild type (10.01 ±0.10%), (p=0.023). The Csf1r$^{+/-}$ group didn't show remarkable difference (9.25±1.01%) compared with wild type group (p=0.613). When compared with Csf1r$^{-/-}$ embryos a statistically difference was founded (p=0.036). Regarding epithelial VD, Csf1r$^{-/-}$ and Csf1r$^{+/-}$ embryos showed a significant decrease (42.55±0.87% and 39.19±1.74%, respectively) compared with wild type (51.45±0.92%) (p=0.003 and p=0.001, respectively). At last, concerning airspace VD Csf1r$^{-/-}$ lung embryos presented a mean of 16.17±1.343%, Csf1r$^{+/-}$ of 21.60±2.69% and wild type embryos of 18.11±0.91%. Although a slight increase was observed comparing Csf1r$^{+/-}$ and Csf1r$^{-/-}$ with wild type, no statistical differences were found (p=0.264 and p=0.582, respectively).

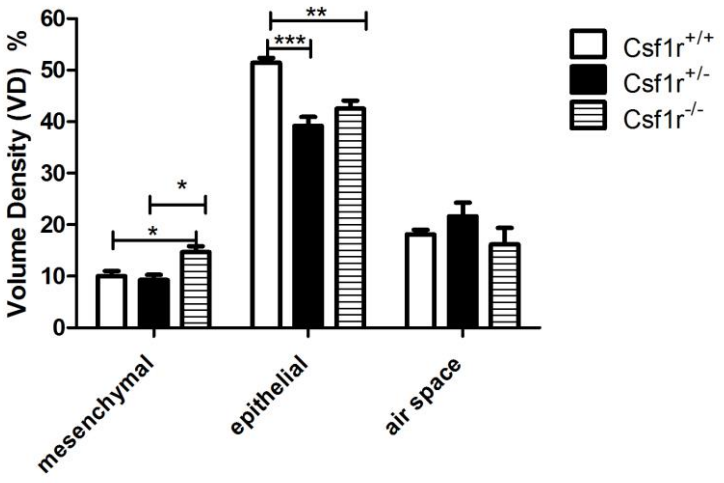

Figure 20. Lung embryos histology at E18.5 stage. Representative pictures of lung histology at E18.5 of Csf1r$^{+/+}$, Csf1r$^{+/-}$ and Csf1r$^{-/-}$ animals. A decrease in epithelial tissue is observed when compared Csf1r$^{+/-}$ and Csf1r$^{-/-}$ with wild type embryos. The Csf1r$^{-/-}$ animals shows also an increase in mesenchymal tissue compared with wild type group.

3.2.3. Lung vasculature

We assessed the vessel density at E18.5 stage in order to understand if lung vasculature was affected by macrophage deletion and an apparent decrease in the number of CD31 positive vessels was observed in Csf1r$^{+/-}$ and Csf1r$^{-/-}$ compared with wild type (**figure 21**).

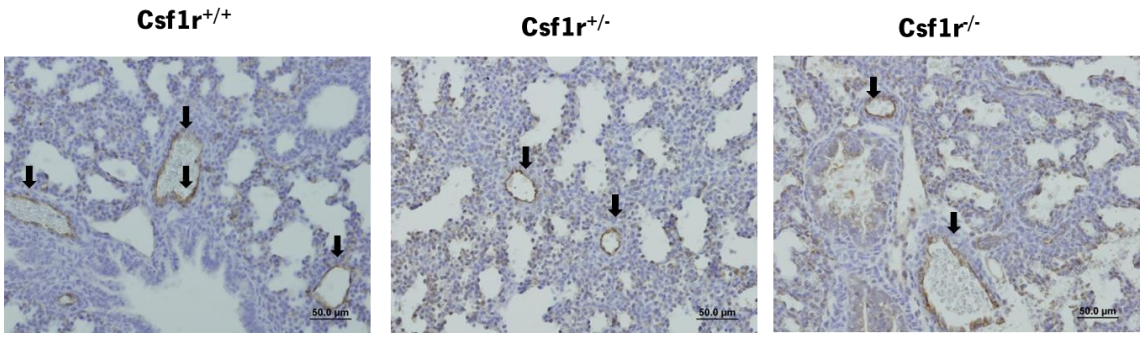

Figure 21. CD31 immunohistochemical staining in lung embryos at E18.5. The CD31 endothelial cell marker was used to stain blood vessels specific cells, endothelial cells (black arrows). A decrease in the number of vessels for knockout animals was found at this stage. Magnification: 20x.

In order to evaluate if the previous vessel structure observations resembled a real impact in the number of vessels, the vessel density was calculated for the different genotypes. The vessel density was determined by counting CD31 positive vascular structures and the results are below (**figure 22**). At E18.5 stage, Csf1r$^{+/-}$ shows a median vessel density of 2.64±0.19, Csf1r$^{-/-}$ of 2.52±0.25 and wild type of 3.29±0.36. Therefore, knockout animals shows a decrease in the number of vessels compared with control, however without statistically significant differences (Csf1r$^{+/-}$ vs wild type p=0.132, and Csf1r$^{-/-}$ vs wild type p=0.188).

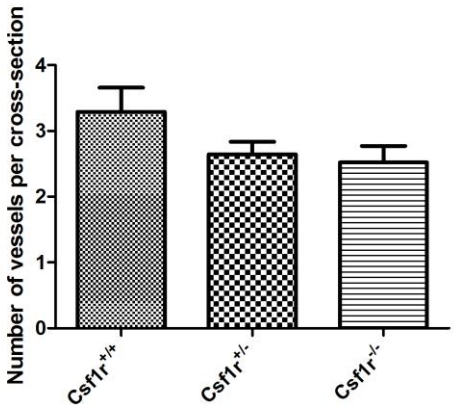

Figure 22. Vessel Density quantification at E 18.5. Vessel density was determined by counting CD31 positive vascular structures. Knockout animals (Csf1r$^{+/-}$ and Csf1r$^{-/-}$) showed a decrease in the number of vascular structures. n= 5 of Csf1r$^{+/+}$; n=6 of Csf1r$^{+/-}$ and n=3 of Csf1r$^{-/-}$ lung animals were analyzed. Data is represented as mean ± SEM.

3.2.4. Gene expression of angiogenic factors

We performed a transcripts levels quantification of the following angiogenic factors: VEGF-A, Flk-1, Ang-1, Ang-2, HIF-1a and Fgf2, at E18.5 stage (**figure 23**).

Regarding VEGF-A expression fold change $Csf1r^{+/-}$ and $Csf1r^{-/-}$ lungs presented 0.67±0.067 and 0.65±0.086, respectively, compared with wild type (1.00±0.055), with statistically significant differences (p=0.002 and p=0.005), respectively.

Flk-1, also showed this trend, with $Csf1r^{+/-}$ showing a median fold decrease of 0.93±0.074, $Csf1r^{-/-}$ of 0.86±0.080 comparing the control (1.00±0.060). However, no statistical differences were obtained (p values>0.050). Ang-1 expression levels were similar in knockout ($Csf1r^{+/-}$ of 1.00±0.056 and $Csf1r^{-/-}$ of 1.09±0.064) compared with wild type lungs (1.00±0.039), with no statistical differences (p values>0.050).

To Ang-2, the median fold change of $Csf1r^{+/-}$ was 0.89±0.027, $Csf1r^{-/-}$ 0.78±0.060 having wild type as reference (1.00±0.047). Therefore, a significant decrease in the expression of Ang-2 was found for $Csf1r^{-/-}$ animals comparing with wild type (p=0.025), but not for $Csf1r^{+/-}$ (p=0.119).

Regarding, HIF-1α the fold change of $Csf1r^{+/-}$ (0.97±0.044), $Csf1r^{-/-}$ (1.05±0.058) and wild-type (1.00±0.033) was similar. Therefore, no differences were found in the gene expression levels (p>0.400). At last, Fgf2 gene expression levels didn't show statistical differences (p>0.400); with the median fold change of $Csf1r^{+/-}$ of 1.023±0.065, $Csf1r^{-/-}$ of 1.045±0.066 and wild type of 1.00±0.025.

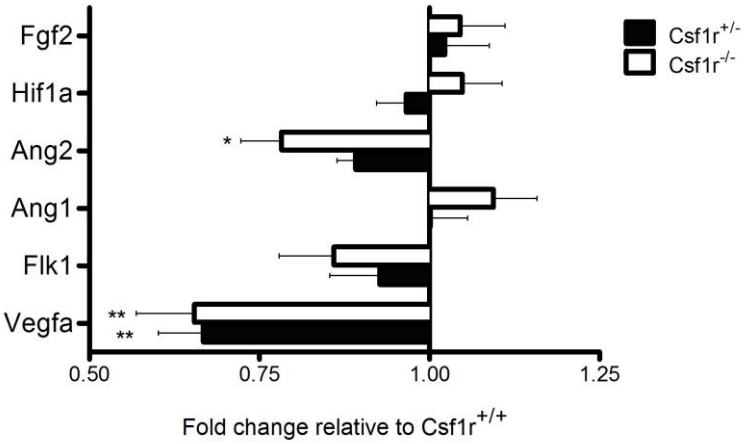

Figure 23. Angiogenic factors gene expression profile by qPCR of lung at E 18.5. Comparison of VEGF-A, Flk-1, Ang-1, Ang-2, HIF-1a and Fgf2 gene expression between $Csf1r^{+/-}$ and $Csf1r^{-/-}$ with $Csf1r^{+/+}$ animals. All genes were normalized against GADPH expression. Lungs analyzed: n= 10 of $Csf1r^{+/+}$; n=7 of $Csf1r^{+/-}$; n=4 of $Csf1r^{-/-}$. *p<0.050;**p<0.010

3.2.5. Arterial thickness

The previous results suggest that the macrophage-deficient-mice present a deficient vasculature. Thus, we performed complementary evaluation specifically about the arteries structures. The comparison between the artery thicknesses between the different genotypes trough the representative pictures didn't evidence differences (**figure 24**). In order to check this apparent similar thickness, the measurement of the arteries thickness was performed (**figure 25**). The artery thickness was determined by the measurement of distance between external and internal elastic fibers. The $Csf1r^{+/-}$ animals showed a median of artery thickness of 2.571± 0.220, $Csf1r^{-/-}$ of 2.808±0.318 and wild type of 2.789± 0.220. The results didn't showed significant differences ($Csf1r^{+/-}$ vs wild type p=0.492, $Csf1r^{-/-}$ vs wild type p=0.959, between knockouts p=0.550).

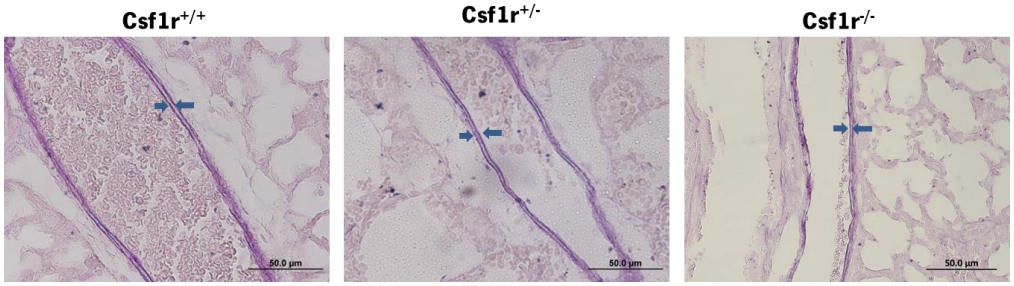

Figure 24. Arterial thickness at E18.5 stage. Comparison between $Csf1r^{+/+}$, $Csf1r^{+/-}$ and $Csf1r^{-/-}$ animals. The results didn't shows remarkable differences between the three genotypes. Arrows point the elastic fibers in purple that highlight the characteristic structure of these blood vessels: the tunica intima (more internal elastic lamina), the tunica media (between the two elastic laminas) and the tunica adventitia (blending in with lung airways). Magnification: 40 xs.

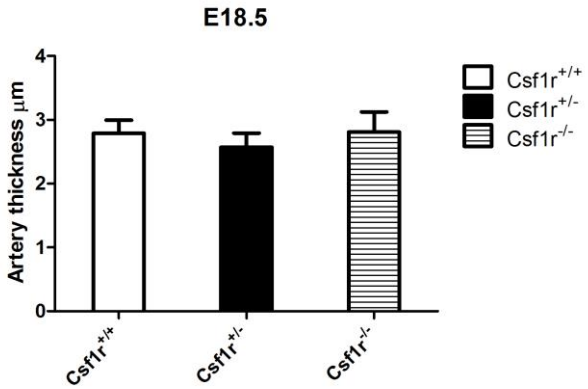

Figure 25. Arterial thickness evaluation at E18.5 stage. Comparison between the artery thickness of $Csf1r^{+/+}$, $Csf1r^{+/-}$ and $Csf1r^{-/-}$ animals. The results didn't shows remarkable differences between the three genotypes. Data is represented as mean ± SEM.

3.3. Impact of macrophages deletion in post-natal saccular stage of lung development (P0)

3.3.1. Lung gross morphology

In order to evaluate if macrophages deletion results in a visible disruption in the development of post-natal murine lungs, the gross morphology was analyzed after birth (P0). The correspondent pictures are represented above (**figure 26**). The knockouts mutant embryos, $Csf1r^{+/-}$ and $Csf1r^{-/-}$, didn't showed gross differences in size and aspect when compared with wild type.

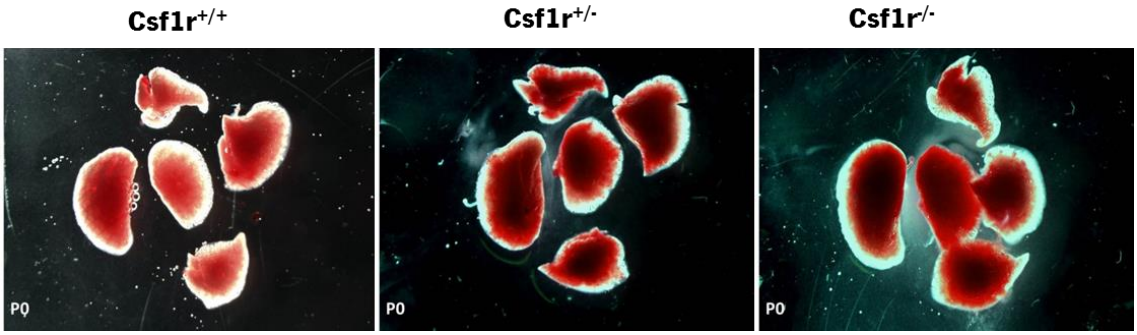

Figure 26. Gross morphology evaluation of lung newborns at P0 stage. Above are represented the illustrative lung pictures immediately after dissection at P0 stage. No gross differences in size, shape and morphology were found between $Csf1r^{+/-}$ and $Csf1r^{-/-}$ and wild type lungs. Magnification: 0.7x.

3.3.2. Lung-to-body weight ratios

In order to understand if macrophage deletion results in lung hypoplasia, the left, right and total lung-to-body weight ratio were calculated for the different genotypes (**figure 27**). The results didn't shows remarkable differences between the knockouts and wild type animals. For left lung-to-body ratio the $Csf1r^{+/-}$ animals showed a median of 0.0081± 0.0005, $Csf1r^{-/-}$ of 0.0102±0.0009 and wild type 0.0089± 0.0010, with no statistical differences ($Csf1r^{+/-}$ vs wild type p=0.404, $Csf1r^{-/-}$ vs wild type p=0.406, between knockouts p=0.043). For the right lung-to-body ratio, $Csf1r^{+/-}$ animals showed a mean of 0.0161± 0.0005, the $Csf1r^{-/-}$ 0.0197±0.0019 and wild type 0.0174± 0.0008, with statistical differences only between the knockouts animals (p=0.024). For the total lung-to-body ratio, similar tendencies were observed, with the knockout

lungs presenting a significant difference (p=0.015) (mean: Csf1r$^{+/-}$ 0.0242±0.0008, Csf1r$^{-/-}$ 0.0299±0.0026 and wild type 0.0263± 0.0016).

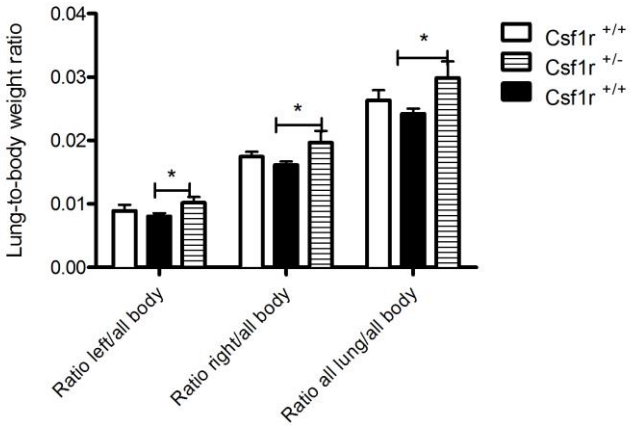

Figure 27. Left, right and total lung-to-body weight ratio at P0 stage. Comparison of left, right and total lung by all body weight between Csf1r$^{+/+}$, Csf1r$^{+/-}$ and Csf1r$^{-/-}$ animals. The results didn't show differences between the knockout and wild type mice. *p <0.050

3.3. Neonatal blood gasometry

In order to understand if the alterations on vascular component results in an impairment of respiratory capacity, it was performed blood gasometric evaluation immediately after birth. The blood was collected after decapitation and gasometric evaluation of pH, partial pressure of CO_2, O_2 (PCO_2 and PO_2 respectively), as well saturation of O_2 (Sat O_2) and Lactate concentration (Lac) was performed. Concerning pH, no differences were found between the tree genotypes (p>0.100).

When compared with control, knockout neonates presented a slight increase in PCO_2 and PO_2, with no statistical differences (p>0.050). Regarding $SatO_2$, again no differences were found between the tree genotypes (p>0.200). Lastly, when compared with control, Csf1r$^{-/-}$ neonates presented an increase in lactate values. However, no statistical difference was observed (p>0.050).

Table 1. Neonatal blood gasometric evaluation after birth

	pH	PCO_2 (mmHg)	PO_2 (mmHg)	$SatO_2$ (%)	Lac (mmol/L)
Csf1r$^{+/+}$	7.64±0.03	28.30±3.15	48.00±5.86	89.33±5.17	2.36±0.55
Csf1r$^{+/-}$	7.51±0.06	39.98±4.11	62.40±12.26	88.20±5.84	1.57±0.49
Csf1r$^{-/-}$	7.58±0.02	37.40±1.30	62.00±13.00	93.00±4.00	3.23±1.33

P- partial pressure; Sat- saturation. Values represent the mean ±SEM of measurements.

3.3.4. Lung morphology

The histological pictures of lung morphogenesis at P0 stage are showed below in **figure 28**. No apparent differences in lung morphogenesis were observed in wild type versus Csf1r$^{+/-}$ newborn. However, when compared the wild type versus Csf1r$^{-/-}$ animals, the knockout lungs were severely hypoplastic with greatly increased mesenchymal cellularity and reduced epithelial tissue. Also, pre-alveoli were greatly reduced when compared with wild type embryos, which presented a defined network of air change. Additionally, the air space was reduced in Csf1r$^{-/-}$ lung embryos. Indeed, the morphogenesis of Csf1r$^{-/-}$ lungs appeared to be delayed at more early stage of development.

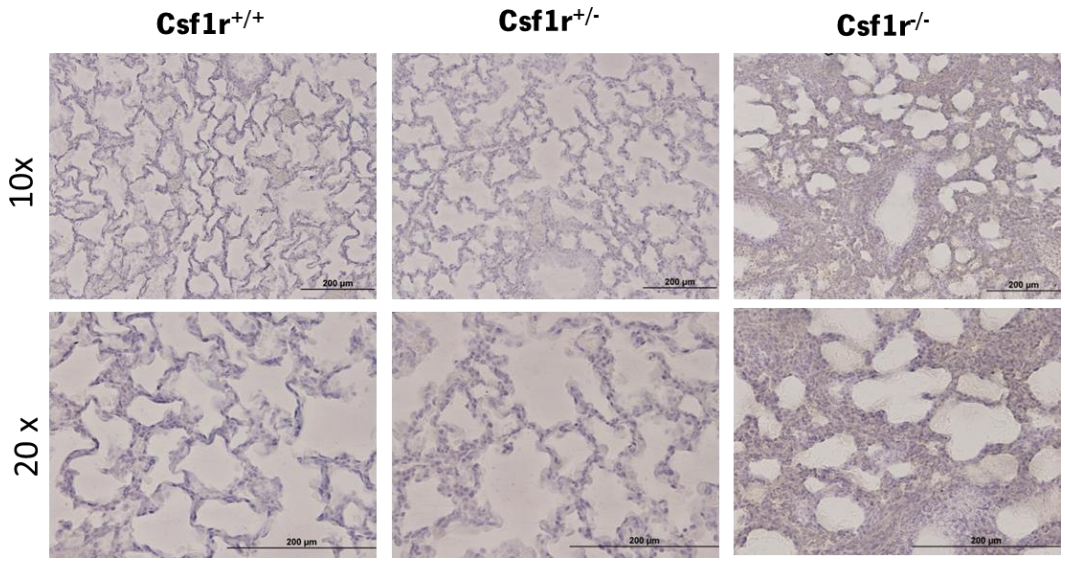

Figure 28. Lung histology at P0 stage. Representative pictures of lung histology of Csf1r$^{+/+}$, Csf1r$^{+/-}$ and Csf1r$^{-/-}$ animals at P0 stage. Reduced air space and increased cellularity in Csf1r$^{-/-}$ animals compared either with Csf1r$^{+/-}$ and the control is clearly visible. These animals showed an increase in mesenchymal tissue, a decrease in air space and epithelial area. Magnification: top panel 10 x, bottom panel 20x.

Next, to determine the extension of these observations in mutant animals ($Csf1r^{-/-}$), stereological analyze was performed. At P0 stage, beyond the morphometric measurements of mesenchymal and air space VD, it was also calculated the small (epithelial and septum) and large (bronchiolar) epithelium (**figure 29**). The quantification results showed that large epithelium VD of $Csf1r^{-/-}$ lung was significantly reduced (0.21±0.02%) compared with wild type newborns (1.33±0.16%) (p=0.002). Regarding small epithelium VD, $Csf1r^{-/-}$ newborns showed a minor increase (28.56±5.42%) compared with wild type (22.53±1.62%) (p=0.327). Concerning mesenchymal VD, $Csf1r^{-/-}$ lung newborns showed a mean of 9.49±2.21%, $Csf1r^{+/-}$ of 1.12±0.49% and wild type of 1.34±0.88%. A great increase was found in $Csf1r^{-/-}$ comparing with wild type (p=0.014) and comparing with $Csf1^{+/-}$ (p= 0.004). Between $Csf1^{+/-}$ and wild type no remarkable differences were found (p=0.820). Finally, regarding air space, $Csf1r^{-/-}$ lung newborns showed mean of 31.45±2.73%, $Csf1r^{+/-}$ 45.97±2.09% and wild type (53.24±4.95%). Therefore, a significant decrease in $Csf1r^{-/-}$ animals was found (p=0.008).

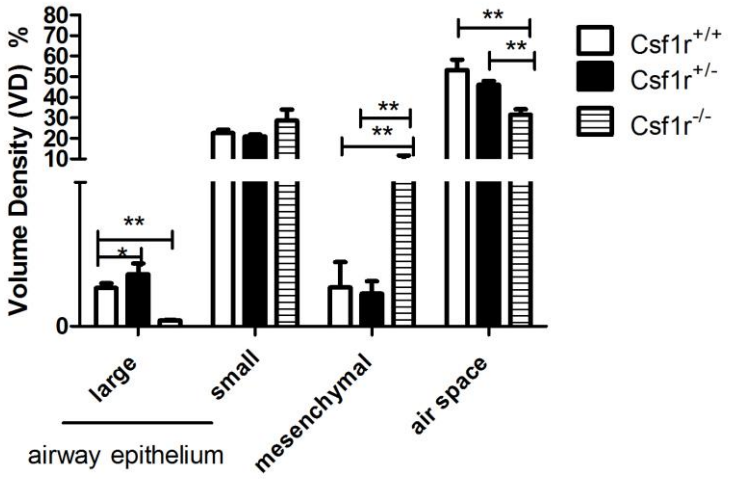

Figure 29. Sterelogical analyses at P0 developmental stage. Above are represented the stereological results of mesenchymal, epithelial (large and small airways) and air space volume density. n=4 for $Csf1r^{+/+}$, n= 5 $Csf1r^{+/-}$ and n=4 for $Csf1r^{-/-}$ group. The large epithelium showed a decrease in $Csf1r^{-/-}$ animals. The mesenchymal VD was higher in $Csf1r^{-/-}$ lungs when compared with wild type. The air space VD was lesser in knockout animals. Data is represented as mean ± SEM. *p<0.050**p<0.010

3.3.5. Lung vasculature

We assessed lung vessel structure at P0 stage in order to understand if vessel number was affected. An apparent decrease in the number of CD31 positive vessels were found in Csf1r$^{+/-}$ and Csf1r$^{-/-}$ compared with control (**figure 30**).

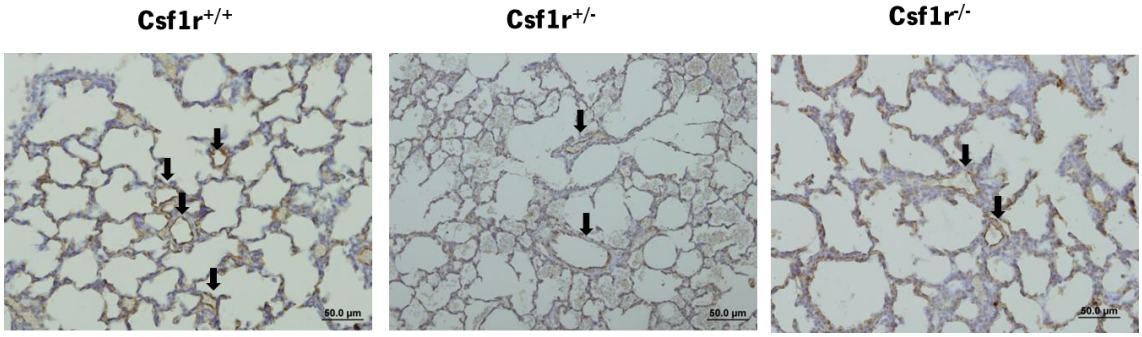

Figure 30. CD31 immunohistochemical staining in lung embryos at P0 stage. The CD31 endothelial cell marker was used to stain blood vessels specific cells, endothelial cells (black arrows). A decrease in the number of vessels for knockout animals was observed. Magnification: 20x.

In order to evaluate if the previous subjective analysis of vessel constitution corresponded to a real impact in the number of vessels; the vessel density was calculated for the different groups. The vessel density was determined by counting CD31 positive vascular structures and the results are below (**figure 31**). At P0 stage, Csf1r$^{+/-}$ showed a median of 2.54±26, Csf1r$^{-/-}$ of 2.22±0.15 and wild type of 3.76±0.32. Therefore, knockout animals exhibited almost a two-fold decrease in vessel density compared with wild type (Csf1r$^{+/-}$ vs wild type p=0.016 and Csf1r$^{-/-}$ vs wild type p=0.002).

3.3.6. Gene expression of angiogenic factors

We performed a quantification of transcript levels of relevant angiogenic factors (VEGF-A, Flk-1, Ang-1, Ang-2, HIF-1a and Fgf2) (**figure 32**).

At P0 stage, Csf1r$^{+/-}$ lungs showed median VEGF-A expression fold changes of 1.81±0.125, Csf1r$^{-/-}$ of 1.68±0.223 with wild type as reference (1.00±0.160). Therefore, both knockout animals showed a significant increase in the expression levels of VEGF-A (Csf1r$^{+/-}$ vs wild type p=0.001 and Csf1r$^{-/-}$ vs wild type p=0.033). In VEGR-2, this trend was also observed, with a

median fold change of Csf1r$^{+/-}$ 1.59±0.116, Csf1r$^{-/-}$ 1.58±0.193 and wild-type 1.00±0.107. Therefore, gene expression levels of Flk-1 were 59 and 58% higher in Csf1r$^{+/-}$ (p=0.002) and Csf1r$^{-/-}$ (p=0.016), respectively, comparing with wild type. Concerning Ang-1, Csf1r$^{+/-}$ shows a median fold change of 5.52±0.918, Csf1r$^{-/-}$ of 5.03±1.993 and wild type of 1.00±0.192. Therefore, knockout animals presented a significant high increase in Ang-1 transcript levels (Csf1r$^{+/-}$ vs wild type p=0.001 and Csf1r$^{-/-}$ vs wild type p=0.012. On the other hand, only Csf1r$^{-/-}$ showed fold increase in Ang-2 expression (2.16±0.412 vs 1.10±0.080 in Csf1r$^{+/-}$ and 1.00±0.088 in wild-type), with statistical differences (p=0.001). Concerning HIF-1a, a median fold change of 1.06±0.039 in Csf1r$^{+/-}$, 1.25±0.154 in Csf1r$^{-/-}$ was observed. No statistical differences were found (p>0.050). Additionally, no statistical differences were observed in Fgf2 change expression levels (p>0.050), with Csf1r$^{+/-}$ presenting a median of 1.10±0.065, Csf1r$^{-/-}$ of 1.09±0.105 and wild type of 1.00±0.180.

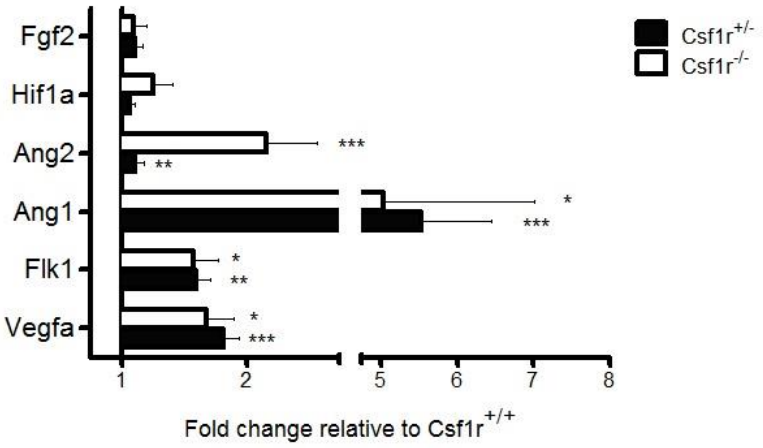

Figure 31. Angiogenic factors gene expression profile by qPCR of lung newborns at P0. Comparison of VEGF-A, Flk-1, Ang-1, Ang-2, HIF-1a and Fgf2 gene expression between Csf1r$^{-/-}$ and Csf1r$^{-/-}$ with Csf1r$^{+/+}$ animals.. All genes were normalized against GADPH expression. . Lungs analyzed: n= 9 of Csf1r$^{+/+}$; n=13 of Csf1r$^{+/-}$; n=2 of Csf1r$^{-/-}$. *p<0.050;**p<0.010

3.3.7. Arterial thickness

The previous results suggest that the macrophage-deficient-mice can show pulmonary hypertension, since the up regulation of VEGF-Flk1 pathway is verified. In this pathology the increase in artery thickness is a characteristic point [98]. Therefore, the alteration of artery thickness could be used as an indirect pulmonary hypertension assessment. The comparison

between the artery thicknesses between the genotypes trough the representative pictures didn't showed differences (**figure 33**). In order to check this apparent similar thickness, the measurement of the arteries thickness was performed (**figure 34**). The results didn't showed considerable differences. The Csf1r$^{+/-}$ animals showed a mean of 2.727±0.195, Csf1r$^{-/-}$ of 2.627±0.209 and wild type of 2.377±0.219 (p>0.050).

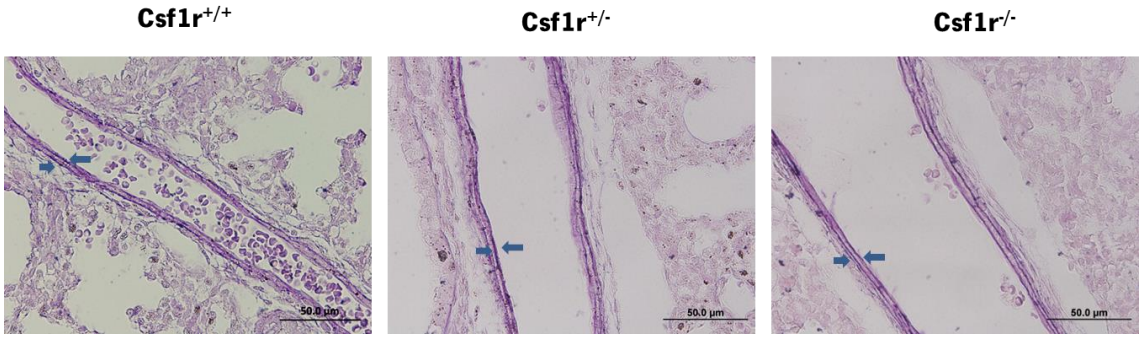

Figure 32. Arterial thickness at P0 stage. Comparison between Csf1r$^{+/+}$, Csf1r$^{+/-}$ and Csf1r$^{-/-}$ animals. The results didn't shows remarkable differences between the three genotypes. . Arrows point the elastic fibers in purple that highlight the characteristic structure of these blood vessels: the tunica intima (more internal elastic lamina), the tunica media (between the two elastic laminas) and the tunica adventitia (blending in with lung airways). Magnification: 40 xs.

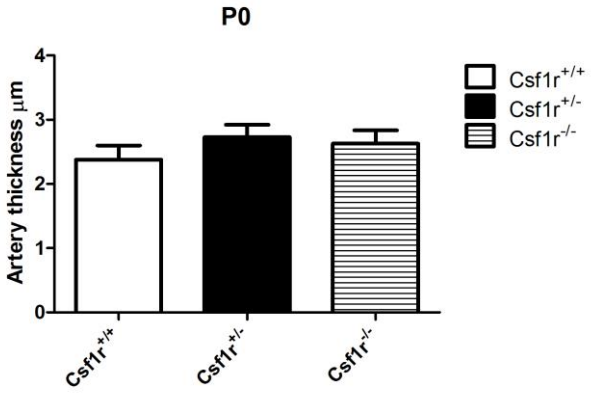

Figure 33. **Arterial thickness evaluation at P0 stage.** Comparison between the artery thickness of Csf1r$^{+/+}$, Csf1r$^{+/-}$ and Csf1r$^{-/-}$ animals. The results didn't shows remarkable differences between the three genotypes. Data is represented as mean ± SEM.

DISCUSSION

4. DISCUSSION

Nowadays it becomes increasingly clear that macrophages have a higher heterogeneity of functions, which are beyond immune context. Their close association with the development in organs such as brain [73], pancreas [81], mammary gland [55], kidney [99], among others has already been demonstrated. Moreover, some studies have demonstrated the regulation of developmental morphogenesis by macrophages, as in vascular system formation and branching morphogenesis [24]. Lung is a branching organ and its morphogenesis is dependent on interactions between epithelial and endothelial compartments. In fetal lung, macrophages are present in mesenchyme throughout all developmental stages, representing around 5% of the total lung cells at E15.5 stage and their number increase significantly during post-natal period [31]. However, their function and the consequences of macrophage ablation during lung development remain unknown.

The present work characterizes, for the first time, the effect of macrophage ablation in the mice lung development process, using a macrophage-deficient mice model, Csf1r$^{-/-}$. Since the disruption of the *Csf1r* gene results in large depletion of macrophages in most of tissues, it is a good model to study trophic roles played by these cells in the development of organ and systems [31]. The lung morphology evaluation was accessed by the measurement of histological compartments, through stereological analyses. Considering that macrophages have already been linked to the angiogenesis in other organs and the crucial relevance of vascular process in lung, the present work also addresses the relevance of this population in the regulation of lung vasculature, through evaluation of vessel density and of angiogenic factors expression levels.

Having in mind that macrophage ablation can disrupt lung development, as logical approach, we studied the morphology of knockout (Csf1r$^{+/-}$ and Csf1r$^{-/-}$) per comparison with wild type animals. Concerning gross morphology results, the knockout animals didn't show gross development abnormalities comparing with control. Also newborn knockout mice didn't showed alterations on left, right and total lung-to-body weight ratio, which are indicators of pulmonary hypoplasia. Nevertheless, the close association of macrophages and the branching process in organs such as kidney [99], mammary gland [55] and pancreas [81] led us to investigate if the branching process was affected in knockout animals at E15.5 stage. The results didn't shows significant alterations on peripheral airway buds number for both knockout animals comparing with wild

type group. However, the number of wild type animals analyzed (n=2) didn't allow establishing a definitive conclusion, being necessary to increase the number of animals analyzed.

Regarding histological evaluation, the Csf1r$^{-/-}$ lungs at pseudoglandular stage showed an increase in mesenchymal tissue comparing with wild type and Csf1r$^{+/-}$. This fact points out to an impairment of lung development due to macrophages ablation, since the arrest on lung development is characterized by an increase in mesenchyme tissue [100]. Furthermore, epithelial and air space compartments seems also to be impaired, although without significant differences. At fetal saccular stage, beyond the increase in the mesenchyme, a significant reduction in epithelial component was observed in Csf1r$^{-/-}$ animals. This finding reinforces the question addressed in this work: a deficiency in lung development, namely delay in tissue differentiation, due to lack of tissue macrophages. At post-natal saccular stage, again the mesenchymal component was increased. The opposite tendency was displayed in large airways (bronchiolar) epithelium, with Csf1r$^{-/-}$ presenting a significantly decreased in comparison with wild type animals. Moreover, the same trend was found to airspace. These findings indicate that tissue macrophages are an important cellular component in the lung morphogenesis, through different lung developmental stages, and their ablation is sufficient to cause a delay in lung development. However, it remains to establish which main drivers determine this impairment. It's known that lung morphogenesis depends on epithelial-mesenchymal interactions that are governed by numerous growth and transcription factors regulating cell proliferation, differentiation and death [101]. Moreover, macrophages are important players in all referred process [101]. Moreover, macrophages are important players in all referred process [102]. In lung these events are coordinated by a large number of signaling molecules, such as bone morphogenetic proteins (BMP), fibroblast growth factors (FGF), Wnt/β-catenin, among others [101]. All described factors could constitute important targets to be evaluated, allowing to explain the delay found in the development of macrophage-deficient mice. On the other hand, it is known, that structural maturation facilitates the progressive gain in gas exchange efficiency [103], what means that this delay of lung development could result in impairment on lung function. In this way, the lung functionality constituted a rational target to be assessed by gasometry evaluation.

The gasometry results showed that, while pH values were relatively stable, the partial pressure of the carbon dioxide (PO_2) was increased in knockout animals. Normally, the combination of lowered pH values and increased PCO_2 levels are indicators of respiratory acidosis consistent with respiratory function alteration [104]. Therefore, the increase in PCO_2 reveals a possible alteration

in respiratory (capacity respiration disorders and with lowered ventilation). Regarding pH, this is determined by a reason between hydrogen carbonate (HCO_3) and CO_2 and the increase of partial pressure of CO_2 results in an increase in [H^+] leading to an increase of pH [105]. An increase in PCO_2 was showed in knockout animals but these animals didn't showed changes in pH, as would be expected. This could be explained by compensatory mechanisms occurring to balance this parameter. In agreement with data from the literature, when an acid-base disturbance develops, the modulation of various body buffer pairs allows the maintenance of pH levels. For instance, phosphate, hemoglobin, and other proteins, including albumin, change in protonated and unprotonated concentrations. The organism will then try to correct the extracellular pH towards normal [106]. Oxygen deficiency in the organism favours the anaerobic metabolism increasing the lactic acid production and decrease of blood's pH production [107] which didn't occurred in macrophage-deficient mice. The increase of lactate production is associated with oxygen deficiency, but the levels of oxygen are similar for all genotypes [107]. The preliminary results didn't showed significant alterations of pH, PO_2, PCO_2, $SatO_2$ and lactate levels in macrophage-deficient mice. Nevertheless, the level of PCO2 increases (almost significant value) in these animals, which can suggests a possible impact in lung function, since the increase of this parameter is a strong indicator of lung inefficient function. However, the number of knockout animals analysed was smaller, being necessary to increase it to allow establish definitive conclusions.

Our second goal was to understand whether tissue macrophage ablation impairs vascular lung development. It has been demonstrated that during organ development and remodelling, macrophages support angiogenesis, not only by the expression of proangiogenic factors and matrix-remodelling proteases, but also by the physical interaction with vessels [108]. Also, one close link between endothelial and epithelial component drives the lung development. Particularly, inhibition of lung endothelial cell development is accompanied by inhibition of airway epithelial cell differentiation and maturation [13]. Thus, we hypothesize that macrophage ablation, trough the Csf1r deletion, may disrupt lung vascular development, compromising the lung development. Our results showed a significant decrease in the vessel number of macrophage deficient-mice lungs at post-natal saccular stage. This clear impairment in endothelial structure can be associated with morphological alterations described above in epithelial/mesenchymal compartments., the interaction between endothelial and epithelial/mesenchymal compartments is crucial in lung morphogenesis [109]. Lung vascular

orchestration is governed at early stages for angiogenesis and vasculogenesis processes. Specifically, the coordination of pro- and anti- angiogenic signals is required for the normal development of vascular network in different organs [14]. A large number of molecules are known as regulators of angiogenesis. However, it is assumed that the signaling cascade involving vascular endothelium factor (VEGF) is the critical pathway in this process since, this growth factor is a powerful inducer of angiogenesis in a large number of experimental models *in vivo* and *in vitro* [110] [111]. VEGF-A is a potent inducer of angiogenesis, being a survival factor that prevents the apoptosis of endothelial cells [97]. Importantly, in lung VEGF-A is a central growth factor regulating physiological and pathological lung formation [13]. Indeed, lung is one of the organs with the highest expression of VEGF in animal systems [20]. Flk-1 is the main mediator of VEGF-A effect. The activation of Flk1 stimulates a number of signal transduction pathways responsible for mitogenesis, migration, and survival of endothelial cells [97]. Our results showed that at pseudoglandular stage (E15.5) the activation of this crucial pro-angiogenic pathway in knockout animals. By contrast, at fetal saccular stage (E18.5), the opposite trend was observed with a down regulation of this pathway. At post-natal saccular stage (P0) the VEGF-A/Flk-1 pathway was newly up regulated.

Another important signalling pathway in vascular development is the Tie2/Ang system. While Ang-1 triggers Tie2 phosphorylation, stimulating angiogenesis, Ang-2 binds but does not activate Tie2, being a competitive inhibitor of Ang-1 [112]. At pseudoglandular stage a strong increase of Ang-2 was found. The opposite trend was observed at fetal saccular stage (E18.5), with the down regulation of this factor. Again, at post-natal saccular stage (P0) this angiopoietin was up regulated. It's known that the activity of Ang-2 is normally anti-angiogenic.Thus, the up regulation found in Ang-2 would not be expected, either at pseudoglandular, as well at post-natal saccular stage. However, the effect of Ang2 on angiogenesis depends on the presence of VEGF: in the absence of VEGF, Ang2 induces vascular regression, but when VEGF is present, Ang-2 induces angiogenesis, promoting vessel sprouting by blocking a constitutive Ang-1 signal [112]. The positive or negative Ang2 action is consequently dependent of VEGF-A signal. Therefore, the higher levels of Ang-2 could have a stimulatory angiogenic effect in macrophage-deficient mice lungs due to VEGF-A increase. Regarding Hif1-a, this factor belongs to hypoxia-inducible factor (HIF) family, which comprises three different transcription factors HIF-1, HIF-2 and HIF-3 [113]. HIF-1 is a heterodimeric protein composed of two subunits, an oxygen-inducible subunit, HIF-1a, and a constitutively expressed one, HIF-1β [114] [115]. In absence of oxygen, HIF-1a directly

activates the transcription of the vascular endothelial growth factor (VEGF) gene and the one of its receptor, vascular endothelial growth factor receptor 1 (VEGFR-1) [116]. In all studied stages no remarkable differences were found, suggesting that the regulation of oxygen levels remains unaltered. As VEGF family, Fgf-2 is a potent angiogenesis inducer in vivo and in vitro, increasing the formation of new blood vessels [117]. In addition to a direct effect on endothelial cells, Fgf-2 has stimulatory effect in VEGFA. Combined stimulation of Fgf2 and VEGFA angiogenic molecules has been associated with synergistic effects on neovascular formation in experimental conditions both in vivo and in vitro, increasing intercellular communication, which leads to mural cell recruitment and formation of mature vessels [118]. At pseudoglandular stage significant increase in Fgf2 was found. At this stage a up regulation of VEGF-A, Flk-1, Ang-2 and Fgf2, suggest that macrophage ablation leads to a stimulation of angiogenic activity, perhaps due to some compensation mechanisms trying to reverse the delay in lung development, demonstrated by an increase in mesenchymal tissue by stereological analysis. The opposite trend was demonstrated at fetal saccular stage (E18.5) with a down regulation of VEGF-A/Flk-1 pathway. In opposition of the results showed at E15.5 stage, these results suggest that macrophage ablation regulates negatively the angiogenic activity. The reverse of this phenotype was found at post-natal saccular stage with a significant increase in the transcripts expression levels of VEGFA, Flk-1, Ang-1 and Ang-2 demonstrating the stimulation of angiogenic activity. At pseudoglandular stage regarding vessel density, the results showed a minor increase of the vessel number in the knockout animals compared with control, which is consistent with a stimulatory effect of the up regulation of mentioned pro angiogenic factors. At fetal saccular stage the vessel density was slight decreased in macrophage-deficient mice and again consistent with the down regulation of pro angiogenic factors and therefore with reserve of angiogenic activity. Likely, at this stage the effort to try reverse the morphological impairment showed was not enough. Possible because the vascular density begins to be affected, still without significance, and the angiogenic activity is down regulated. At least, at post-natal saccular stage (P0) the angiogenic activity was increase by the up regulation of pro angiogenic factors. However, the poor vascular constitution showed at this stage become the previous results unexpected. One possible explanation could be the continue impairment in lung vasculature from fetal to post-natal saccular stage, which leads the system to try reverse this delay increasing the pro-angiogenic activity. Moreover, this tendency is already observed in adult lung pathologic contexts. For example, lungs from patients with severe forms of pulmonary hypertension a strong VEGF expression in the angioproliferative plexiform

lesions was found [119] [120] [121]. In mice, VEGF gene and protein expression is upregulated in the lung tissue after disease induction by hypoxic exposition [122]. In rat lung, mRNA levels for both VEGF and Flk-1 were increased using hypoxia-induced pulmonary hypertension (PH) [123]. The PH is characterized by an increase thickness of media and adventitia of pulmonary arterial walls [98]. Regarding the findings of this work demonstrating the impairment in vasculature and in angiogenic factors expression profile in macrophage deficient mice, the artery structure assessment constitutes a logic parameter to evaluate. However, no alterations in artery thickness were found in knockout compared with wild type mice, in any of the developmental stages evaluated. Therefore, these evidences indicate no influence of tissue macrophages in arterial walls constitution, a classical feature of PH.

The angiogenic balance is also important in epithelial morphogenesis. For instance, the main VEGF-Flk1 pathway role is on vascular system, but also it is also involved in the regulation of pulmonary epithelial morphogenesis, namely during alveorization, once type II pneumocytes and bronchiolar epithelial cells produce VEGF and express their receptors [13, 124]. It was demonstrated that exogenous addiction of VEGF in human fetal lung induces airway epithelial cell proliferation. Moreover, overexpression of VEGFA in peripheral epithelial cells leads to lung dysmorphogenesis [125] [126]. On the other hand, disruption of VEGFA signaling results in a delay of airspace maturation [124], retardation of alveolarization as well as a reduction on capillary number [127], being the capillary network essential for alveolar formation [96]. All described facts, can support the strong disruption found in morphology at post-natal stage, since the coordinated construction of airway epithelial and endothelial lung cell compartments requires a VEGF gradient, which is disrupted at this stage [20].

Together, these results suggest that macrophage ablation is critical to lung development impairing airway epithelial and vascular compartments. Moreover, the close interaction between these two systems to the normal lung formation could explain the results of both, vascular and epithelial parts.

To date, the understanding of lung macrophage function have been focused on pathological contexts namely in inflammation over showing their contribution during lung development. This study identifies tissue macrophages as critical players during lung development.The present work characterizes, for the first time, the effect of macrophage ablation on mice lung development. At least, at three different stages macrophage-deficient mice showed impairment of lung development in both compartments: airways and vasculature. These findings

open a wide perspective for future new targets to be evaluated during lung development. The improvement on the understanding of the role of macrophages in lung development regulation has potential clinical relevance, since macrophage modulation could be a target to promote lung development, mainly in pathological contexts, such as congenital pulmonary diseases.

.

FUTURE PESPECTIVES

5. FUTURE PERSPECTIVES

Our previous results showed a strong delay during lung development in macrophage-deficient mice. Macrophages contribute to development through apoptosis, phagocytic and removal of cellular debris and as strong effector cells producing a variety of trophic factors, which stimulate growth and control cellular differentiation. Therefore, the effect of macrophage ablation in proliferation, differentiation and cell death it's a key target to be evaluated.

As future perspective, also the extensive characterization of macrophage population during fetal lung development should be performed, quantitatively and qualitatively. Because, although the number and macrophage profile during post-natal development has been described by other groups, the number of macrophages during fetal development and also the precise known about how the macrophages subtypes interfere with its development remains unknown.

In lung, during branching morphogenesis, macrophages are located abundant and densely located within branch points. And it is known that many of the intercellular signaling networks controlling the morphogenesis of branched tubular organs are conserved in the respiratory system. Therefore, an interesting approach could be the use a co-culture of lung explants with M1 and M2 polarized macrophages and the evaluation of branching process.

BIBLIOGRAPHY

6. BIBLIOGRAPHY

1. Morrisey, E.E. and B.L. Hogan, *Preparing for the first breath: genetic and cellular mechanisms in lung development.* Dev Cell, 2010. **18**(1): p. 8-23.
2. Chinoy, M.R., *Lung growth and development.* Front Biosci, 2003. **8**: p. d392-415.
3. Ghadiali, S. and Y. Huang, *Role of airway recruitment and derecruitment in lung injury.* Crit Rev Biomed Eng, 2011. **39**(4): p. 297-317.
4. Rawlins, E.L., *The building blocks of mammalian lung development.* Dev Dyn, 2011. **240**(3): p. 463-76.
5. Cardoso, W.V. and J.A. Whitsett, *Resident cellular components of the lung: developmental aspects.* Proc Am Thorac Soc, 2008. **5**(7): p. 767-71.
6. Keijzer, R. and P. Puri, *Congenital diaphragmatic hernia.* Semin Pediatr Surg, 2010. **19**(3): p. 180-5.
7. Shannon, J.M. and B.A. Hyatt, *Epithelial-mesenchymal interactions in the developing lung.* Annu Rev Physiol, 2004. **66**: p. 625-45.
8. Groenman, F., S. Unger, and M. Post, *The molecular basis for abnormal human lung development.* Biol Neonate, 2005. **87**(3): p. 164-77.
9. Center, C.C.s.H.M. *Pulmonary Biology - Lung morphogenesis*. 1999 [cited 08-03-2013]; Available from: http://www.cincinnatichildrens.org/research/divisions/p/pulmonary-bio/lung-morphogenesis/.
10. Rock, J.R. and B.L. Hogan, *Epithelial progenitor cells in lung development, maintenance, repair, and disease.* Annu Rev Cell Dev Biol, 2011. **27**: p. 493-512.
11. Zhou, L., et al., *Thyroid transcription factor-1, hepatocyte nuclear factor-3beta, surfactant protein B, C, and Clara cell secretory protein in developing mouse lung.* J Histochem Cytochem, 1996. **44**(10): p. 1183-93.
12. Que, J., et al., *Mesothelium contributes to vascular smooth muscle and mesenchyme during lung development.* Proceedings of the National Academy of Sciences, 2008. **105**(43): p. 16626-16630.
13. Crivellato, E., *The role of angiogenic growth factors in organogenesis.* Int J Dev Biol, 2011. **55**(4-5): p. 365-75.
14. Chung, A.S. and N. Ferrara, *Developmental and pathological angiogenesis.* Annu Rev Cell Dev Biol, 2011. **27**: p. 563-84.
15. Stenmark, K.R. and S.H. Abman, *Lung vascular development: implications for the pathogenesis of bronchopulmonary dysplasia.* Annu Rev Physiol, 2005. **67**: p. 623-61.
16. Vadivel, A., et al., *Critical role of the axonal guidance cue EphrinB2 in lung growth, angiogenesis, and repair.* Am J Respir Crit Care Med, 2012. **185**(5): p. 564-74.
17. Wilkinson, G.A., et al., *Role for ephrinB2 in postnatal lung alveolar development and elastic matrix integrity.* Dev Dyn, 2008. **237**(8): p. 2220-34.
18. Du, L., et al., *Signaling Molecules in Nonfamilial Pulmonary Hypertension.* New England Journal of Medicine, 2003. **348**(6): p. 500-509.
19. Taichman, D.B., et al., *Notch1 and Jagged1 expression by the developing pulmonary vasculature.* Dev Dyn, 2002. **225**(2): p. 166-75.
20. Voelkel, N.F., R.W. Vandivier, and R.M. Tuder, *Vascular endothelial growth factor in the lung.* American Journal of Physiology - Lung Cellular and Molecular Physiology, 2006. **290**(2): p. L209-L221.
21. Gerber, H.P., et al., *VEGF is required for growth and survival in neonatal mice.* Development, 1999. **126**(6): p. 1149-59.

22. Del Moral, P.-M., et al., *VEGF-A signaling through Flk-1 is a critical facilitator of early embryonic lung epithelial to endothelial crosstalk and branching morphogenesis.* Developmental Biology, 2006. **290**(1): p. 177-188.
23. Zeng, X., et al., *VEGF enhances pulmonary vasculogenesis and disrupts lung morphogenesis in vivo.* Dev Dyn, 1998. **211**(3): p. 215-27.
24. Pollard, J.W., *Trophic macrophages in development and disease.* Nat Rev Immunol, 2009. **9**(4): p. 259-70.
25. Lloyd, C.M., et al., *Three-colour fluorescence immunohistochemistry reveals the diversity of cells staining for macrophage markers in murine spleen and liver.* Journal of Immunological Methods, 2008. **334**(1–2): p. 70-81.
26. Song, L., C. Lee, and C. Schindler, *Deletion of the murine scavenger receptor CD68.* J Lipid Res, 2011. **52**(8): p. 1542-50.
27. Austyn, J.M. and S. Gordon, *F4/80, a monoclonal antibody directed specifically against the mouse macrophage.* European Journal of Immunology, 1981. **11**(10): p. 805-815.
28. Rhein, P., et al., *CD11b is a therapy resistance– and minimal residual disease–specific marker in precursor B-cell acute lymphoblastic leukemia.* Blood, 2010. **115**(18): p. 3763-3771.
29. Bertrand, J.Y., et al., *Three pathways to mature macrophages in the early mouse yolk sac.* Blood, 2005. **106**(9): p. 3004-11.
30. Hume, D.A., *The mononuclear phagocyte system.* Curr Opin Immunol, 2006. **18**(1): p. 49-53.
31. Rae, F., et al., *Characterisation and trophic functions of murine embryonic macrophages based upon the use of a Csf1r-EGFP transgene reporter.* Dev Biol, 2007. **308**(1): p. 232-46.
32. Lichanska, A.M., et al., *Differentiation of the mononuclear phagocyte system during mouse embryogenesis: the role of transcription factor PU.1.* Blood, 1999. **94**(1): p. 127-38.
33. Dzierzak, E., A. Medvinsky, and M. de Bruijn, *Qualitative and quantitative aspects of haematopoietic cell development in the mammalian embryo.* Immunol Today, 1998. **19**(5): p. 228-36.
34. van Furth, R., et al., *The mononuclear phagocyte system: a new classification of macrophages, monocytes, and their precursor cells.* Bull World Health Organ, 1972. **46**(6): p. 845-52.
35. DeKoter, R.P., J.C. Walsh, and H. Singh, *PU.1 regulates both cytokine-dependent proliferation and differentiation of granulocyte/macrophage progenitors.* EMBO J, 1998. **17**(15): p. 4456-4468.
36. Pixley, F.J. and E.R. Stanley, *CSF-1 regulation of the wandering macrophage: complexity in action.* Trends Cell Biol, 2004. **14**(11): p. 628-38.
37. Yeung, Y.G. and E.R. Stanley, *Proteomic approaches to the analysis of early events in colony-stimulating factor-1 signal transduction.* Mol Cell Proteomics, 2003. **2**(11): p. 1143-55.
38. Bourette, R.P. and L.R. Rohrschneider, *Early events in M-CSF receptor signaling.* Growth Factors, 2000. **17**(3): p. 155-66.
39. Hamilton, J.A., *CSF-1 signal transduction.* J Leukoc Biol, 1997. **62**(2): p. 145-55.
40. Hamilton, J.A., *Colony-stimulating factors in inflammation and autoimmunity.* Nat Rev Immunol, 2008. **8**(7): p. 533-44.
41. Fortier, A.H. and L.A. Falk, *Isolation of murine macrophages.* Curr Protoc Immunol, 2001. **Chapter 14**: p. Unit 14 1.
42. Pollard, J.W. and E.R. Stanley, *Pleiotropic Roles for CSF-1 in Development Defined by the Mouse Mutation Osteopetrotic*, in *Advances in Developmental Biochemistry*, M.W. Paul, Editor. 1996, Academic Press. p. 153-193.

43. Lin, H., et al., *Discovery of a cytokine and its receptor by functional screening of the extracellular proteome.* Science, 2008. **320**(5877): p. 807-11.
44. Sica, A. and A. Mantovani, *Macrophage plasticity and polarization: in vivo veritas.* J Clin Invest, 2012. **122**(3): p. 787-95.
45. Martinez, F.O., et al., *Macrophage activation and polarization.* Front Biosci, 2008. **13**: p. 453-61.
46. Ezekowitz, R.A. and S. Gordon, *Alterations of surface properties by macrophage activation: expression of receptors for Fc and mannose-terminal glycoproteins and differentiation antigens.* Contemp Top Immunobiol, 1984. **13**: p. 33-56.
47. Mosser, D.M. and E. Handman, *Treatment of murine macrophages with interferon-gamma inhibits their ability to bind leishmania promastigotes.* J Leukoc Biol, 1992. **52**(4): p. 369-76.
48. Mantovani, A., *Macrophage diversity and polarization: in vivo veritas.* Blood, 2006. **108**(2): p. 408-409.
49. Murray, P.J. and T.A. Wynn, *Protective and pathogenic functions of macrophage subsets.* Nat Rev Immunol, 2011. **11**(11): p. 723-37.
50. Lebre, M.C., Tak, P.P., *Macrophage Subsets in Immune-Mediated Inflammatory Disease: Lessons from Rheumatoid Arthritis, Spondyloarthritis, Osteoarthitis, Behçet's Disease and Gout.* The Open Arthritis Journal, 2010. **3**: p. 18-23.
51. Hume, D., *The Biology of Macrophages - An Online Review.* 2012 [cited 09-06-2013]; Available from: http://www.macrophages.com/macrophage-review.
52. Perry, V.H., D.A. Hume, and S. Gordon, *Immunohistochemical localization of macrophages and microglia in the adult and developing mouse brain.* Neuroscience, 1985. **15**(2): p. 313-26.
53. Sasmono, R.T., et al., *A macrophage colony-stimulating factor receptor-green fluorescent protein transgene is expressed throughout the mononuclear phagocyte system of the mouse.* Blood, 2003. **101**(3): p. 1155-63.
54. Cecchini, M.G., et al., *Role of colony stimulating factor-1 in the establishment and regulation of tissue macrophages during postnatal development of the mouse.* Development, 1994. **120**(6): p. 1357-72.
55. Schwertfeger, K.L., J.M. Rosen, and D.A. Cohen, *Mammary gland macrophages: pleiotropic functions in mammary development.* J Mammary Gland Biol Neoplasia, 2006. **11**(3-4): p. 229-38.
56. Geutskens, S.B., et al., *Macrophages in the murine pancreas and their involvement in fetal endocrine development in vitro.* J Leukoc Biol, 2005. **78**(4): p. 845-52.
57. Dougall, W.C., et al., *RANK is essential for osteoclast and lymph node development.* Genes & Development, 1999. **13**(18): p. 2412-2424.
58. Wiktor-Jedrzejczak, W., et al., *Total absence of colony-stimulating factor 1 in the macrophage-deficient osteopetrotic (op/op) mouse.* Proc Natl Acad Sci U S A, 1990. **87**(12): p. 4828-32.
59. Van Wesenbeeck, L., et al., *The osteopetrotic mutation toothless (tl) is a loss-of-function frameshift mutation in the rat Csf1 gene: Evidence of a crucial role for CSF-1 in osteoclastogenesis and endochondral ossification.* Proc Natl Acad Sci U S A, 2002. **99**(22): p. 14303-8.
60. Grey, A., et al., *Evidence for a Functional Association between Phosphatidylinositol 3-Kinase and c-src in the Spreading Response of Osteoclasts to Colony-Stimulating Factor-1.* Endocrinology, 2000. **141**(6): p. 2129-2138.
61. Begg, S.K., et al., *Delayed hematopoietic development in osteopetrotic (op/op) mice.* The Journal of Experimental Medicine, 1993. **177**(1): p. 237-242.
62. Lin, E.Y., et al., *The macrophage growth factor CSF-1 in mammary gland development and tumor progression.* J Mammary Gland Biol Neoplasia, 2002. **7**(2): p. 147-62.

63. Schwertfeger, K.L., et al., *A critical role for the inflammatory response in a mouse model of preneoplastic progression.* Cancer Res, 2006. **66**(11): p. 5676-85.
64. Gouon-Evans, V., M.E. Rothenberg, and J.W. Pollard, *Postnatal mammary gland development requires macrophages and eosinophils.* Development, 2000. **127**(11): p. 2269-82.
65. Van Nguyen, A. and J.W. Pollard, *Colony Stimulating Factor-1 Is Required to Recruit Macrophages into the Mammary Gland to Facilitate Mammary Ductal Outgrowth.* Developmental Biology, 2002. **247**(1): p. 11-25.
66. Maffei, M., et al., *Increased expression in adipocytes of ob RNA in mice with lesions of the hypothalamus and with mutations at the db locus.* Proc Natl Acad Sci U S A, 1995. **92**(15): p. 6957-60.
67. Cohen, P.E., et al., *Macrophages: important accessory cells for reproductive function.* J Leukoc Biol, 1999. **66**(5): p. 765-72.
68. Cohen, P.E., M.P. Hardy, and J.W. Pollard, *Colony-stimulating factor-1 plays a major role in the development of reproductive function in male mice.* Mol Endocrinol, 1997. **11**(11): p. 1636-50.
69. Bulloch, K., et al., *CD11c/EYFP transgene illuminates a discrete network of dendritic cells within the embryonic, neonatal, adult, and injured mouse brain.* J Comp Neurol, 2008. **508**(5): p. 687-710.
70. Cohen, P.E., et al., *Colony-stimulating factor 1 regulation of neuroendocrine pathways that control gonadal function in mice.* Endocrinology, 2002. **143**(4): p. 1413-22.
71. Kondo, Y., C.A. Lemere, and T.J. Seabrook, *Osteopetrotic (op/op) mice have reduced microglia, no Abeta deposition, and no changes in dopaminergic neurons.* J Neuroinflammation, 2007. **4**: p. 31.
72. Erblich, B., et al., *Absence of colony stimulation factor-1 receptor results in loss of microglia, disrupted brain development and olfactory deficits.* PLoS One, 2011. **6**(10): p. e26317.
73. Michaelson, M.D., et al., *CSF-1 deficiency in mice results in abnormal brain development.* Development, 1996. **122**(9): p. 2661-72.
74. Vilhardt, F., *Microglia: phagocyte and glia cell.* Int J Biochem Cell Biol, 2005. **37**(1): p. 17-21.
75. Lalancette-Hebert, M., et al., *Selective ablation of proliferating microglial cells exacerbates ischemic injury in the brain.* J Neurosci, 2007. **27**(10): p. 2596-605.
76. Diez-Roux, G., et al., *Macrophages kill capillary cells in G1 phase of the cell cycle during programmed vascular regression.* Development, 1999. **126**(10): p. 2141-7.
77. Lobov, I.B., et al., *WNT7b mediates macrophage-induced programmed cell death in patterning of the vasculature.* Nature, 2005. **437**(7057): p. 417-21.
78. Rao, S., et al., *Obligatory participation of macrophages in an angiopoietin 2-mediated cell death switch.* Development, 2007. **134**(24): p. 4449-58.
79. Fantin, A., et al., *Tissue macrophages act as cellular chaperones for vascular anastomosis downstream of VEGF-mediated endothelial tip cell induction.* Blood, 2010. **116**(5): p. 829-40.
80. Colen, K.L., et al., *Vascular development in the mouse embryonic pancreas and lung.* J Pediatr Surg, 1999. **34**(5): p. 781-5.
81. Banaei-Bouchareb, L., et al., *Insulin cell mass is altered in Csf1op/Csf1op macrophage-deficient mice.* J Leukoc Biol, 2004. **76**(2): p. 359-67.
82. Brain, J.D., *Mechanisms, measurement, and significance of lung macrophage function.* Environ Health Perspect, 1992. **97**: p. 5-10.
83. Lehnert, B.E., *Pulmonary and thoracic macrophage subpopulations and clearance of particles from the lung.* Environ Health Perspect, 1992. **97**: p. 17-46.
84. Nicod, L.P., *Pulmonary defence mechanisms.* Respiration, 1999. **66**(1): p. 2-11.

85. Zhang, P., et al., *Innate immunity and pulmonary host defense.* Immunol Rev, 2000. **173**: p. 39-51.
86. Crowell, R.E., et al., *Alveolar and interstitial macrophage populations in the murine lung.* Exp Lung Res, 1992. **18**(4): p. 435-46.
87. Blackwell, T.S., et al., *NF-kappaB signaling in fetal lung macrophages disrupts airway morphogenesis.* J Immunol, 2011. **187**(5): p. 2740-7.
88. Jones, C.V., et al., *M2 macrophage polarisation is associated with alveolar formation during postnatal lung development.* Respir Res, 2013. **14**: p. 41.
89. Nogueira-Silva, C., et al., *Leukemia inhibitory factor in rat fetal lung development: expression and functional studies.* PLoS One, 2012. **7**(1): p. e30517.
90. Nogueira-Silva, C., et al., *IL-6 is constitutively expressed during lung morphogenesis and enhances fetal lung explant branching.* Pediatr Res, 2006. **60**(5): p. 530-6.
91. Bartram, U. and C.P. Speer, *THe role of transforming growth factor β in lung development and disease*.* CHEST Journal, 2004. **125**(2): p. 754-765.
92. Jaskoll, T., P.D. Boyer, and M. Melnick, *Tumor necrosis factor-alpha and embryonic mouse lung morphogenesis.* Dev Dyn, 1994. **201**(2): p. 137-50.
93. Jobe, A.J., *The New BPD: An Arrest of Lung Development.* Pediatr Res, 1999. **46**(6): p. 641-641.
94. Weibel, E.R., C.C. Hsia, and M. Ochs, *How much is there really? Why stereology is essential in lung morphometry.* J Appl Physiol, 2007. **102**(1): p. 459-67.
95. Livak, K.J. and T.D. Schmittgen, *Analysis of relative gene expression data using real-time quantitative PCR and the 2(-Delta Delta C(T)) Method.* Methods, 2001. **25**(4): p. 402-8.
96. Hislop, A.A., *Airway and blood vessel interaction during lung development.* J Anat, 2002. **201**(4): p. 325-34.
97. Karamysheva, A.F., *Mechanisms of angiogenesis.* Biochemistry (Mosc), 2008. **73**(7): p. 751-62.
98. Mohseni-Bod, H. and D. Bohn, *Pulmonary hypertension in congenital diaphragmatic hernia.* Semin Pediatr Surg, 2007. **16**(2): p. 126-33.
99. Lee, S., et al., *Distinct macrophage phenotypes contribute to kidney injury and repair.* J Am Soc Nephrol, 2011. **22**(2): p. 317-26.
100. El-Hashash, A.H.K., et al., *Six1 transcription factor is critical for coordination of epithelial, mesenchymal and vascular morphogenesis in the mammalian lung.* Developmental Biology, 2011. **353**(2): p. 242-258.
101. Cardoso, W.V. and J. Lu, *Regulation of early lung morphogenesis: questions, facts and controversies.* Development, 2006. **133**(9): p. 1611-24.
102. Stefater, J.A., 3rd, et al., *Metchnikoff's policemen: macrophages in development, homeostasis and regeneration.* Trends Mol Med, 2011. **17**(12): p. 743-52.
103. Bolender, R.P., D.M. Hyde, and R.T. Dehoff, *Lung morphometry: a new generation of tools and experiments for organ, tissue, cell, and molecular biology.* American Journal of Physiology - Lung Cellular and Molecular Physiology, 1993. **265**(6): p. L521-L548.
104. Schwarzkopf, T.M., et al., *Blood gases and energy metabolites in mouse blood before and after cerebral ischemia: the effects of anesthetics.* Exp Biol Med (Maywood), 2013. **238**(1): p. 84-9.
105. Vengust, M., *Hypercapnic respiratory acidosis: a protective or harmful strategy for critically ill newborn foals?* Can J Vet Res, 2012. **76**(4): p. 275-80.
106. Seifter, J.L., *Chapter 113 –ACID-BASE DISORDERS.* Cecil Textbook of Medicine, 2004.
107. Wajs, W., et al., *Predictive Analysis of Blood Gasometry Parameters Related to the Infants Respiration Insufficiency*, in *Computational Science – ICCS 2006*, V. Alexandrov, et al., Editors. 2006, Springer Berlin Heidelberg. p. 300-307.

108. Nucera, S., D. Biziato, and M. De Palma, *The interplay between macrophages and angiogenesis in development, tissue injury and regeneration.* Int J Dev Biol, 2011. **55**(4-5): p. 495-503.
109. Burri, P.H., *Fetal and postnatal development of the lung.* Annu Rev Physiol, 1984. **46**: p. 617-28.
110. Gerber, H.P., et al., *Vascular endothelial growth factor regulates endothelial cell survival through the phosphatidylinositol 3'-kinase/Akt signal transduction pathway. Requirement for Flk-1/KDR activation.* J Biol Chem, 1998. **273**(46): p. 30336-43.
111. Benjamin, L.E., et al., *Selective ablation of immature blood vessels in established human tumors follows vascular endothelial growth factor withdrawal.* J Clin Invest, 1999. **103**(2): p. 159-65.
112. Maisonpierre, P.C., et al., *Angiopoietin-2, a natural antagonist for Tie2 that disrupts in vivo angiogenesis.* Science, 1997. **277**(5322): p. 55-60.
113. Rankin, E.B. and A.J. Giaccia, *The role of hypoxia-inducible factors in tumorigenesis.* Cell Death Differ, 2008. **15**(4): p. 678-85.
114. Harris, A.L., *Hypoxia--a key regulatory factor in tumour growth.* Nat Rev Cancer, 2002. **2**(1): p. 38-47.
115. Semenza, G.L., *Hypoxia-inducible factors: mediators of cancer progression and targets for cancer therapy.* Trends Pharmacol Sci, 2012. **33**(4): p. 207-14.
116. Otrock, Z.K., et al., *Hypoxia-inducible factor in cancer angiogenesis: Structure, regulation and clinical perspectives.* Critical Reviews in Oncology/Hematology, 2009. **70**(2): p. 93-102.
117. Seghezzi, G., et al., *Fibroblast growth factor-2 (FGF-2) induces vascular endothelial growth factor (VEGF) expression in the endothelial cells of forming capillaries: an autocrine mechanism contributing to angiogenesis.* J Cell Biol, 1998. **141**(7): p. 1659-73.
118. Kano, M.R., et al., *VEGF-A and FGF-2 synergistically promote neoangiogenesis through enhancement of endogenous PDGF-B-PDGFRbeta signaling.* J Cell Sci, 2005. **118**(Pt 16): p. 3759-68.
119. Geiger, R., et al., *Enhanced expression of vascular endothelial growth factor in pulmonary plexogenic arteriopathy due to congenital heart disease.* J Pathol, 2000. **191**(2): p. 202-7.
120. Hirose, S., et al., *Expression of vascular endothelial growth factor and its receptors correlates closely with formation of the plexiform lesion in human pulmonary hypertension.* Pathol Int, 2000. **50**(6): p. 472-9.
121. Tuder, R.M., et al., *Expression of angiogenesis-related molecules in plexiform lesions in severe pulmonary hypertension: evidence for a process of disordered angiogenesis.* J Pathol, 2001. **195**(3): p. 367-74.
122. Partovian, C., et al., *Heart and lung VEGF mRNA expression in rats with monocrotaline- or hypoxia-induced pulmonary hypertension.* Am J Physiol, 1998. **275**(6 Pt 2): p. H1948-56.
123. Christou, H., et al., *Increased vascular endothelial growth factor production in the lungs of rats with hypoxia-induced pulmonary hypertension.* Am J Respir Cell Mol Biol, 1998. **18**(6): p. 768-76.
124. Tsao, P.N. and S.C. Wei, *Prenatal hypoxia downregulates the expression of pulmonary vascular endothelial growth factor and its receptors in fetal mice.* Neonatology, 2013. **103**(4): p. 300-7.
125. Akeson, A.L., et al., *Temporal and spatial regulation of VEGF-A controls vascular patterning in the embryonic lung.* Dev Biol, 2003. **264**(2): p. 443-55.
126. Waltenberger, J., et al., *Different signal transduction properties of KDR and Flt1, two receptors for vascular endothelial growth factor.* J Biol Chem, 1994. **269**(43): p. 26988-95.

127. Ng, Y.S., et al., *Differential expression of VEGF isoforms in mouse during development and in the adult.* Dev Dyn, 2001. **220**(2): p. 112-21.